



8-2009

An Analysis of Anaerobic Dual-Anode Chambered Microbial Fuel Cell (MFC) Performance

Min Hea Kim

University of Tennessee - Knoxville

Recommended Citation

Kim, Min Hea, "An Analysis of Anaerobic Dual-Anode Chambered Microbial Fuel Cell (MFC) Performance. " Master's Thesis, University of Tennessee, 2009.
http://trace.tennessee.edu/utk_gradthes/40

This Thesis is brought to you for free and open access by the Graduate School at Trace: Tennessee Research and Creative Exchange. It has been accepted for inclusion in Masters Theses by an authorized administrator of Trace: Tennessee Research and Creative Exchange. For more information, please contact trace@utk.edu.

To the Graduate Council:

I am submitting herewith a thesis written by Min Hea Kim entitled "An Analysis of Anaerobic Dual-Anode Chambered Microbial Fuel Cell (MFC) Performance." I have examined the final electronic copy of this thesis for form and content and recommend that it be accepted in partial fulfillment of the requirements for the degree of Master of Science, with a major in Chemical Engineering.

Paul D. Frymier, Major Professor

We have read this thesis and recommend its acceptance:

John Sanseverino, Eric Boder

Accepted for the Council:

Carolyn R. Hodges

Vice Provost and Dean of the Graduate School

(Original signatures are on file with official student records.)

To the Graduate Council:

I am submitting here with a thesis written by Min Hea Kim entitled “An Analysis of Anaerobic Dual-Anode Chambered Microbial Fuel Cell (MFC) Performance.” I have examined the final electronic copy of this thesis for form and content and recommend that it be accepted in partial fulfillment of the requirements for the degree of Master of Science, with a major in Chemical Engineering.

Paul D. Frymier, Major Professor

We have read this thesis
and recommend its acceptance:

John Sanseverino

Eric Boder

Accepted for the Council:

Carolyn R. Hodges
Vice Provost and Dean of the Graduate School

(Original signatures are on file with official student records.)

**An Analysis of Anaerobic Dual-Anode Chambered
Microbial Fuel Cell (MFC) Performance**

A Thesis
Presented for the
Master of Science
Degree
The University of Tennessee, Knoxville

Min Hea Kim
August 2009

Copyright © 2009 by Min Hea Kim
All rights reserved.

DEDICATION

This thesis is dedicated to my God and family, who have encouraged and showed me endless love and support; without their support and patience, I would not be where I am today.

ACKNOWLEDGEMENTS

I would like to express my deepest gratitude to my advisor, Dr. Paul Frymier, for his overwhelming guidance, patience, and the endless hours spent editing this draft. I feel very fortunate to have had him as my advisor, to have had the opportunity to work with him, and to have had his helpful advice for the past two years. He has been always available and willing to have a discussion with me, even on his busiest days. Working with him has made this journey very pleasant, and for that, I am deeply grateful.

An overwhelming thank you goes to my other research advisor, Dr. John Sanseverino. His experience, support, and encouragement have truly made a difference in my journey. Through all the meetings I have had with him, I have always left his office happier, more encouraged and motivated and I am very thankful for that. I would also like to thank Dr. Eric Boder for agreeing to be on my committee, Dr. David Keffer for providing me the opportunity to join the Chemical Engineering Department, and to Dr. David Icove for his whole-hearted help and trust.

Certainly, this journey was not easy, through struggles and successes my fellow group members and I shared disappointments and victories together. Thus, I would like to extend my gratitude to my group members: Ying Wang, Ifeyinwa Iwuchukwu, Donglee Shin, and Scott Moser. Also special thanks to Ying Wang for her endless guidance and assistance.

Friends have always been important to me and thankfully during my journey great friendships were always there. I would like to thank my friends; Donglee Shin, Minjung Jung, Jaewon Lyu, Anna Choi, Heejin Lim, and Jessica Mitchell. They have brought laughter, happiness, and comfort to not only this journey but my life. During my journey it was difficult to

be away from home; I missed my family and friends from my hometown but even though I was way their love and support were always with me.

Last but not least, my love and gratitude go to my parents, Jongyoun and Heesook, for raising me to always striving for excellence, to value my education and for putting my success and happiness before their own. I am also grateful for their unconditional love and support wherever I was; I am thankful to my sister and brother in a law, Minjoo and Todd, for advising me, showing me the path towards success, and for their patience. Their love and encouragement has always been a constant source of comfort to me when times were difficult. I would also like to thank my mentor, Chuck Lester, whose support and prayer were always there for me at the hardest time of my life.

ABSTRACT

Microbial Fuel Cell (MFC) technology utilizes bacterial growth in carbon-containing solutions to generate electricity or hydrogen. For the direct production of electricity, an MFC operates aerobically at the cathode and anaerobically at the anodes. The same basic design can be used with minor changes to produce hydrogen at the cathode by applying an additional overpotential and omitting oxygen from the cathode. In this configuration, the device is called an MEC (Microbial Electrolysis Cell). However, the term “MFC” is frequently used to describe both devices. The primary objectives of this study were to determine optimal operating conditions and to minimize the internal resistance in the MFC in order to improve the reactor performance for power generation or hydrogen production using the organism *Shewanella oneidensis* MR-1. In this study, MFC performance was evaluated under various operating conditions with a modified MFC system architecture called a “Dual-Anode Chambered MFC” which incorporates two anode chambers flanking a single cathode chamber. This design leads to improvements in reactor performance and reduced internal resistance by minimizing electrode separation and providing parallel electrical connectivity, which increases the maximum current the MFC can supply for a given time (mA). These improvements lead to increased maximum specific power output (W/m^3), volumetric hydrogen production rate ($\text{m}^3\text{-H}_2/\text{m}^3\text{-substrate/day}$), and hydrogen yield on substrate ($\text{mol-H}_2/\text{mol-substrate}$). An analysis of reactor performance using the new MFC reactor system included as system variables the size of the electrode surface area, substrate (lactate) concentration (5mM, 10mM, 20mM), substrate flow rate (1ml/min, 3ml/min, 5ml/min), and internal resistance (Ohms) for electricity production. The maximum

volumetric power density of 23.6 W/m^3 (standard deviation: 2.25, error: 1.3) and hydrogen yield of $0.438 \text{ mol-H}_2/\text{mol-substrate}$ were obtained under optimized conditions; these conditions were then used to compare the reactor performance to that of a single-anode chambered MFC. Results indicated that the dual-anode MFC produced power per unit anode volume of 23.6 W/m^3 , about 1.2 times the power of a single-anode MFC (20.2 W/m^3). This was due to the reduction of internal resistance within the dual-anode MFCs. The internal resistance was reduced by 45 %, from 106 Ohms (single-anode) to 58.3 Ohms (dual-anode).

TABLE OF CONTENTS

CHAPTER 1

INTRODUCTION.....	1
-------------------	---

CHAPTER 2

BACKGROUND	2
------------------	---

2.1 Biological Mechanism	2
--------------------------------	---

2.2 Design Structures	4
-----------------------------	---

2.2.1 Electricity Generation	4
------------------------------------	---

2.2.1. A Aqueous-cathode MFCs with PEMs	5
---	---

2.2.2 Hydrogen Production	7
---------------------------------	---

2.2.2. A Microbial Electrolysis Cells: MECs	7
---	---

2.2.2. B MEC Designs	9
----------------------------	---

2.2.2. C MEC Membrane Materials	11
---------------------------------------	----

2.3 Power Density Measurements.....	12
-------------------------------------	----

2.3.1 Power Output Normalized by Electrode Surface Area	13
---	----

2.3.2 Power Output Normalized by Membrane Surface Area	13
--	----

2.3.3 Power Output Normalized by Volume.....	13
--	----

2.4 Internal Resistance.....	14
------------------------------	----

2.4.1 Measuring Internal Resistance	15
---	----

2.5 Preliminary Research	15
--------------------------------	----

2.5.1 Comparison of MFC Reactor Types	17
2.5.1. A Voltage Production	17
2.5.1. B External Resistance	19
CHAPTER 3	21
MATERIALS AND METHODS	21
3.1 Double-Anode Chambered Microbial Fuel Cell (MFC) Construction	21
3.2 MFC Reactor Design Materials and Features.....	23
3.3 Culture and Medium	25
3.4 Hydrogen Production using a Dual-Anode Chambered MEC	26
3.5 Operational Conditions	28
3.5.1 Experimental Variables	29
3.5.2 Experimental Parameters	29
CHAPTER 4	
RESULTS AND DISCUSSION	31
4.1 Dual-Anode Chambered MFCs for Electricity Production	31
4.1.1 Effect of Cathode Surface Area on Power Generation	31
the dual-anode system.....	32
4.1.2 Power generation as a Function of Substrate Concentration	32
4.1.3 Effect of Substrate and Medium Flow Rates on Power Generation	33

4.1.4 Comparison of Single-Anode Chambered and Dual-Anode Chambered MFC	
Performance	35
4.2 Dual-Anode Chambered MECs for Hydrogen Production	40
CHAPTER 5	
CONCLUSIONS	43
LIST OF REFERENCES	44
VITA.....	47

LIST OF TABLES

Table 1: Effect of Cathode Surface Area on Maximum Power Generation with 5 mM Lactate Concentration	32
Table 2: Effect of Cathode Surface Area on Voltage Production with 5 mM Lactate Concentration	32
Table 3: Maximum Power Density Normalized By Different Parameters at Each Lactate Concentration	34

LIST OF FIGURES

Figure 1: Representation of respiratory chain and standard potentials for <i>Paracoccus denitrificans</i> [3].....	3
Figure 2: Representation of Biological Mechanism of Producing Electricity in a Microbial Fuel Cell [3].....	5
Figure 3: Generalized Schematic of MEC [4]	8
Figure 4: Schematic Representation of MEC with a CEM and an AEM [12]	11
Figure 5: Types of MFCs used in the Previous Research - (A) H-type MFC Reactor Design (B) Sandwich-type MFC Reactor Design [Photograph courtesy of Dr. Ying Wang].....	16
Figure 6: Comparison of Operation Efficiency on Voltage Generation between H- type and Sandwich-type Reactors at 500 ohms	18
Figure 7: The Voltage Output and Power Density as a Function of the External Resistance - (A) H-type MFC reactor design (B) sandwich-type MFC reactor design, the power density was normalized by the reactor volume of the anode chamber.....	19
Figure 8: Schematic Diagram of Continuous Flow System of the Dual-Anode Chambered MFC	22

Figure 9: Representation of Mini Dual-Anode Chambered MFC for Electricity

Generation	24
-------------------------	-----------

Figure 10: Representation of a Dual-Anode Chambered MEC for Hydrogen

Production	27
-------------------------	-----------

Figure 11: Schematic Representation of the Experimental Apparatus for Hydrogen

Production [Courtesy of Donglee Shin] – A carrier gas, flowing at 50 ml/min entered cathode chamber of the MFC. Hydrogen produced in the MFC reactor (cathode) was transported to the hydrogen sensor by the carrier gas. Output from the hydrogen sensor was sent to a personal computer via Labview program	28
--	-----------

Figure 12: Representation of Voltage Production at Different Total Cathode Surface

Areas - Comparison Experiments Run In Triplicate	31
---	-----------

Figure 13: Volumetric Power Density at each Lactate Concentration - (A) Maximum

volumetric power density as a function of lactate concentration with error bars and SD based on the maximum power densities in experiments run in triplicate (B) Plot of saturation kinetics using Michaelis-Menten kinetic model with $K_s = 6.15$, $R^2 = 0.902$	34
---	-----------

Figure 14: The Effect of Substrate and Medium Feed Rates on Power Density..... 36

Figure 15: Comparison of Maximum Power Generation on Single-Anode and Dual-Anode Chambered MFCs under Optimized Operational Conditions at 5 ml/min Flow Rate, 10 mM Lactate.....	36
Figure 16: Power Density and Cell Voltage Curves - By switching out the circuit load; we obtain a data set on the cell voltage and the volumetric power density as a function of resistance (A) Single-Anode Chambered MFC (B) Dual-Anode Chambered MFC.....	38
Figure 17: Power Density Generated as a Function of Current - (A) Single-Anode Chambered MFC (B) Dual-Anode Chambered MFC.....	39
Figure 18: Polarization Curves - Cell voltage versus Current to obtain the polarization curve showing the regions of constant voltage drop (A) Single-Anode Chambered MFC (B) Dual-Anode Chambered MFC.....	39

CHAPTER 1

INTRODUCTION

As we head into the future, large portion of energy produced and used in the world will be from sustainable sources due to the world's limited supply of fossil fuels and their impact on environmental and economic changes. Microbial Fuel Cell (MFC) technology generates either electricity or hydrogen from bacterial growth in carbon-containing solutions, including sources of low or negative economic value such as wastewater. When configured for the production of electricity an MFC is similar to a hydrogen fuel cell in design, but uses bacteria instead of hydrogen to create electricity and can simultaneously treat wastewater as well [4]. Currently most MFC research focuses on increasing the power density of the system based on the projected surface area of electrodes and/or the reactor volume, while little research has been done on determining the effects of varying fuel cell components and the parameters of MFC construction on the voltage output. In this research study, a series of dual-anode chambered MFC reactors were designed and constructed to increase the maximum current of the system and to increase the hydrogen production rate ($\text{m}^3\text{-H}_2/\text{m}^3\text{-substrate per day}$) and yield ($\text{mol-H}_2/\text{mol-substrate}$). This design incorporated dual-anode chambers surrounding a single-cathode chamber, which resulted in improvements in the reactor performance, reducing the internal resistance by minimizing electrode separation. Analysis was conducted for experiments where these small MFCs were operated for both power generation and for hydrogen production. A comparison of the reactor performance between single-anode and dual-anode systems using optimized operating conditions was made for different values of the reactor design and operating parameters, such as cathode electrode surface area, substrate concentration, and substrate flow rate.

CHAPTER 2

BACKGROUND

2.1 Biological Mechanism

This section contains an overview of the biological mechanism and the current design structures of MFCs. An MFC uses bacteria to catalyze the conversion of organic matter into electricity by transferring electrons to an electrical circuit [1]. Microorganisms can transfer electrons to the anode electrode in three ways: using exogenous mediators (ones external to the bacterial cell) such as potassium ferricyanide, anthraquinone 2, 6-disulfonic acid, cobalt sepulchrates, and thionine; using endogenous mediators produced by bacteria; or by direct transfer of electrons from the respiratory enzymes (i.e. cytochromes) to the electrode [3]. Exogenous mediators can divert electrons from the respiratory chain by entering the outer cell membrane, becoming reduced, and then leaving in a reduced state to shuttle the electrons to the electrode. The mediator-less MFCs have more commercial application potential than biofuel cells using exogenous mediators because the mediators used in biofuel cells are expensive, potentially toxic to the microorganisms, and are impractical for an open environment [2].

Several metal-reducing bacteria such as *Shewanella oneidensis*, *Shewanella putrefaciens*, *Geobacter sulfurreducens*, *Geobacter metallireducens* and *Rhodospirillum rubrum* are able to generate electricity in a mediator-less MFC [2]. The bacteria present in mediator-less MFCs typically have electrochemically-active redox enzymes such as cytochromes on their outer membrane that can transfer electrons to external materials and therefore do not require exogenous mediators to accomplish electron transfer to an electrode [2]. Figure 1 shows how the voltage recovered in an MFC depends on where electrons exit the chain of respiratory enzymes.

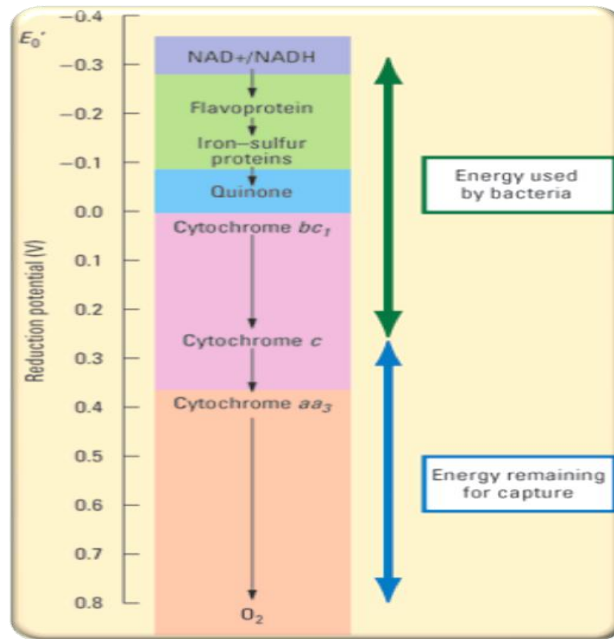


Figure 1: Representation of respiratory chain and standard potentials for *Paracoccus denitrificans* [3]

Bacteria grow by catalyzing chemical reactions, and storing energy in the form of adenosine triphosphate (ATP). Reduced substrates are oxidized and electrons are transferred to respiratory enzymes by NADH. These electrons flow down a respiratory chain which contains a series of enzymes that function to move protons across an internal membrane and create a proton gradient. The protons flow back into the cell through the enzyme ATPase, creating 1 ATP molecule from 1 ADP for every 3 to 4 protons. The electrons are finally released to an electron acceptor. The maximum potential of the process is ~1.2 V, on the basis of the potential difference between the electron carrier and oxygen under standard conditions [3].

Shewanella oneidensis MR-1 is used in this study. *Shewanella oneidensis* MR-1 is a mesophilic, facultative anaerobe that is found mainly in sediment environments [4]. It is capable of utilizing many substrates, including lactate, acetate, pyruvate, serine, and other amino acids

and is capable of reducing a variety of electron acceptors besides oxygen, including Fe(III), Mn(IV), sulfur, nitrate, and fumarate. This organism is called an exoelectrogenic bacterium because it transfers electrons outside the cell via the hypothesized extracellular structure termed nanowires [4]. *Shewanella oneidensis* MR-1 is able to grow both aerobically and anaerobically on a vast array of electron acceptors and plays an important role in metal reduction. Mutagenic and biochemical studies show that *S. oneidensis* reduces ferric iron, a process which involves membrane-bound electron carriers. Lower *et al.* [5] found that anaerobically grown *S. oneidensis* adhered to an iron surface with two to five times greater force than aerobically grown cells, so the observation that this strain was more adhesive under anaerobic conditions might allow closer contact required for electron transfer from cell bound cytochromes even in the absence of nanowires [5]. Bacteria used in an MFC catalyze the conversion of organic matter into electricity [6]. Microorganisms oxidize the substrate and produce electrons and protons in the anode chamber. Electrons, collected on the anode, are transported to the cathode by an external circuit and the protons diffuse through proton exchange membrane (PEM) internally. Electrons and protons are consumed in the cathode chamber by reducing oxygen, usually forming water [7]. In a similar manner, hydrogen gas can be produced at the cathode chamber by applying a small voltage and omitting oxygen from the cathode [8]. A simple representation of the biological mechanism is demonstrated in Figure 2.

2.2 Design Structures

2.2.1 Electricity Generation

In the research literature, a wide range of materials and system designs have been used in MFCs to improve the reactor performance in terms of voltage output, coulombic efficiency, stability,

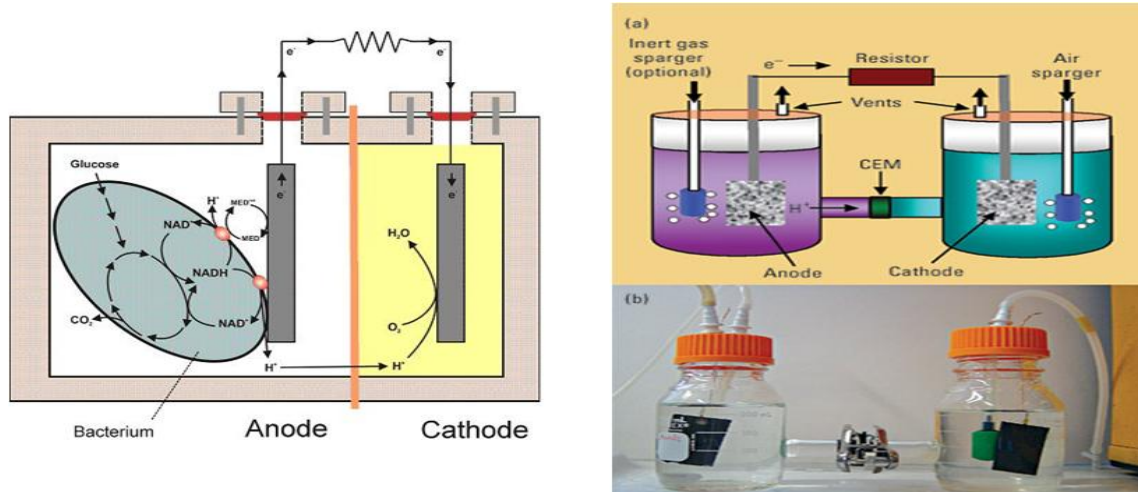


Figure 2: Representation of Biological Mechanism of Producing Electricity in a Microbial Fuel Cell [3]

and longevity. Practical applications of MFCs will require that a design be developed that will not only produce high power and coulombic efficiencies, but one that is also economical to mass produce based on the materials and the reactor architecture.

2.2.1. A Aqueous-cathode MFCs with PEMs

The simplest MFC design such as that in Figure 2 consists of two chambers separated by a PEM. The anode chamber contains a carbon felt electrode, aqueous medium, and the bacterial culture. The cathode chamber contains a platinized carbon cloth electrode with a buffer solution. For electricity generation, the MFC operates aerobically at the cathode side and anaerobically at the anode [3]. In an aqueous cathode chamber, the concentration of dissolved oxygen in the cathode solution can affect MFC performance [3]. Power generation increases when pure oxygen gas is sparged into the cathode and decreases as the dissolved oxygen concentration is lowered. For electricity production the anode chamber is often sparged with nitrogen gas and stir bars are used to provide homogeneous, oxygen-free conditions in the chamber [4]. The PEM membranes

are primarily used in two-chamber MFCs (H-type) as a method for restricting oxygen mass transfer between the liquid-filled anode and cathode chambers; liquid containing dissolved oxygen in the aqueous-cathode cannot be allowed to mix with the bacterial solution in the anode chamber.[4, 12]. However, these H-type MFC reactors have several problems related to the proton transfer efficiency of the PEM which affects the power production including biofouling and oxygen leakage [10]. Chae *et al.* investigated a major problem of oxygen leakage from cathode to anode associated with Nafion PEM membranes. It was found that Nafion PEMs are permeable to oxygen and the oxygen mass transfer coefficient (K_o) and the oxygen diffusion coefficient (D_o) for Nafion PEMs is estimated as $2.80 \times 10^{-4} \text{ cm}^2/\text{s}$ and $5.35 \times 10^{-6} \text{ cm}^2/\text{s}$, respectively when a 50 mM phosphate buffer was used as the catholyte [11]. Chae et al. also found that PEMs operating over long periods of time can be discovered with a biofilm causing adverse effects on mass transport through the membrane [10].

2.2.1. B Air-cathode MFCs without PEMs

Many researchers have chosen to use air-cathode MFCs because of their economical and scalable characteristics; the implementation on site being practical on a large scale (for example, for wastewater treatment), and the affordability of MFC materials [4]. Liu and Logan introduced an air-cathode single chamber MFC lacking a membrane which produced lower coulombic efficiency than an MFC with the membrane, indicating that oxygen diffusion into the anode is increased. It is estimated by Liu and Logan [12], based on oxygen flow rate measurements that oxygen diffusion into the anode chamber with a PEM is much lower than the oxygen diffusion into the anode with the PEM removed. This oxygen is likely consumed by bacteria growing on the cathode instead of the anode in the absence of the PEM [11]. Hence, while potentially being

easier to implement for some large scale applications, membrane-less MFCs suffer from lowered power generation because of the substrate loss due to aerobic oxidation by bacteria on the cathode electrode instead of the anode and loss of efficiency due to a partially aerobic system.

The air-cathode single chamber membrane-less MFC uses a cathode exposed directly to air instead of air-sparged water and theoretically forms an aerobic biofilm on the cathode inner surface (the surface facing the anode) to remove any oxygen that diffuses into the chamber, keeping conditions in the anode chamber anaerobic [12]. However, in practice, this process does not completely eliminate the possibility of an aerobic anode. When only examining the cost of energy production, using an air-cathode single chamber MFC without PEM does help to reduce the material costs by eliminating both the need for energy intensive aeration of the liquid and expensive materials such as a PEM [12]. However, the removal of the PEM increases oxygen transfer into the anode chamber, which is responsible for low electron and energy recoveries in MFCs [13]. While membrane-less MFCs are an interesting research topic, the low electron and energy recoveries make them inefficient [10].

2.2.2 Hydrogen Production

Hydrogen gas can be produced with the same exoelectrogenic bacteria that are used in MFC technology by modifying the MFC design [7]. Biohydrogen production via the electrohydrogenesis process is a recent development, so there are not many systems that have been tested or reported in the literature [4].

2.2.2. A Microbial Electrolysis Cells: MECs

Microbial Electrolysis Cells (MECs, see Figure 3) are based on modifying MFCs in two ways: 1) adding a small voltage (>0.2 V) to the electricity produced by the bacteria and 2)

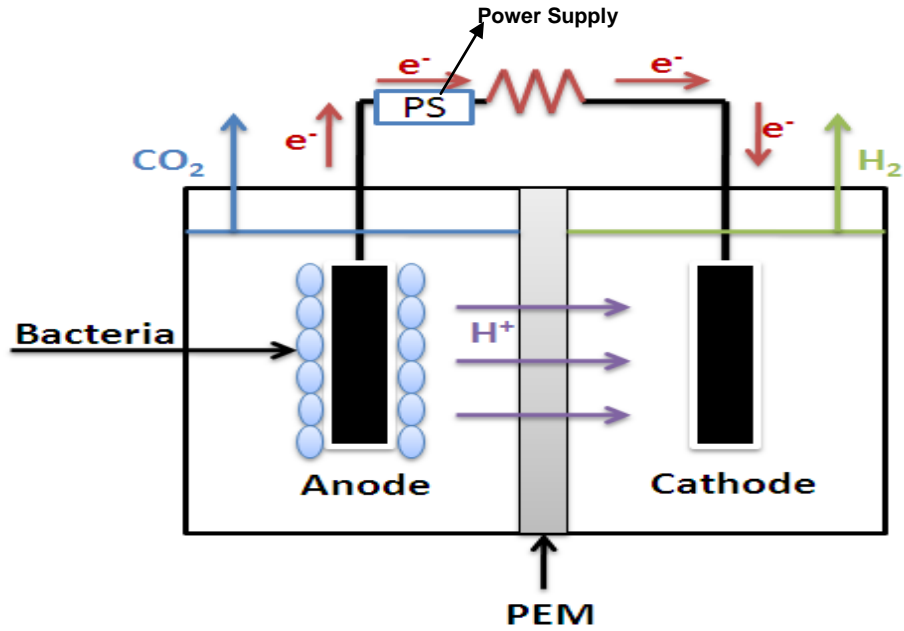


Figure 3: Generalized Schematic of MEC [4]

removing any oxygen at the cathode. In an MFC, an anode potential can approach theoretical limit of $E_{An} = -0.3 \text{ V}$ (e.g. acetate). With oxygen, the cathode potential in an MFC is $\sim 0.2 \text{ V}$, achieving an overall cell voltage $\sim 0.5 \text{ V}$ [$0.2 - (-0.3 \text{ V}) = 0.5 \text{ V}$]. But, in order to form hydrogen gas at the cathode, the oxygen must be removed and overcome a cathode potential at $\text{pH} = 7$ and 298°C of $E_{Cat} = -0.414 \text{ V}$. Therefore, the calculated cell voltage for a system to produce hydrogen at the cathode is $E_{emf} = E_{Cat} - E_{An} = -0.114 \text{ V}$. The cell voltage is negative, so the reaction is not spontaneous and is endothermic. Therefore, in order to overcome this thermodynamic limit for hydrogen evolution, an additional voltage of $>0.114 \text{ V}$ is required [8]. While 0.114 V in theory is needed with acetate as a substrate, in practice larger voltages must be applied due to overpotential at the cathode. In practice, $\sim 0.25 \text{ V}$ or more must be applied to the

circuit to obtain reasonable current densities, and thus hydrogen generation rates [8]. Adding 0.25 V is still substantially less than the voltage needed for water electrolysis, which requires 1.8 to 2.0 V.

It is important for an MEC to operate in a completely anaerobic state in order to produce pure hydrogen [7]. In MECs, protons and electrons released by exoelectrogenic bacteria are recombined to form hydrogen gas instead of forming water at the cathode. A current published study using MEC reports that the biohydrogen gas is produced at yields of 2.01 to 3.95 mol-H₂ per mol-substrate (acetic acid) at an applied voltage of 0.2 to 0.8V. At an applied voltage of 0.6 V, a gas production rate of 1.1m³ H₂ per m³ reactor per day was achieved [14].

2.2.2. B MEC Designs

Call and Logan [8] determined that high hydrogen recovery and production rates are possible in a single chamber MEC without a membrane. In their work, these researchers produced hydrogen gas by using a membrane-less single chamber MEC with a modified design structure including a graphite fiber brush anode and a minimized electrode separation. The hydrogen production rate reaches a maximum of 3.12 m³ H₂ per m³ reactor per day, which is more than double the hydrogen production rate that was obtained in previous studies at an applied voltage of 0.8 V [8].

The same researchers noted that the presence of a membrane (CEM: Cation Exchange Membrane) does not prevent hydrogen diffusion back into the anode chamber [8]. Theoretically, protons are combined equimolarly with electrons at the cathode in biocatalyzed electrolysis ($2\text{H}^+ + 2\text{e}^- \rightarrow \text{H}_2$). They also found that the membrane interrupts proton diffusion by transporting cationic species other than protons [8] and it causes a pH increase in the cathode chamber that

lowers system performance. Increased pH limits bacterial growth at the anode, which in turn limits the hydrogen evolution at the cathode. This pH difference between anode and cathode creates an extra potential loss of about 0.06 V in the system. Similar effects also occur in membrane-less single chamber configuration [15]. These pH gradient related potential losses are more problematic for single chamber configuration (membrane-less) than for two chamber configurations (membrane-present), as ion concentrations increase more rapidly in a single chamber configuration than in the cathode chamber of a two chambered configuration.

Rozendal *et al.* explain that the presence of a membrane in biocatalyzed electrolysis is essential for maintaining the purity of hydrogen gas that is produced at the cathode [9]. By omitting the membrane, the produced hydrogen at the cathode will be contaminated by gaseous metabolic products from the anode chamber such as CO₂, CH₄, H₂S and which will result in a reduction of the coulombic efficiency due to consumption of the hydrogen at the anode chamber [8, 9]. They conclude that the pH increase at the cathode and the potential losses related to the pH gradient across the membrane will occur more rapidly in a single chamber configuration as compared to a double chamber configuration [9]. Additionally, high concentrations of hydrogen gas in the absence of oxygen in a single chamber MEC favors the growth of methanogens which can lower hydrogen recoveries and contaminate the gas with methane [16, 17]. Therefore, as is the case in membrane-less MFCs, a single chamber MEC lacking a membrane suffers from low overall efficiency. In addition, it can create a product gas that is a mixture instead of pure hydrogen. Therefore, there are compelling reasons for developing MECs with membranes.

2.2.2. C MEC Membrane Materials

Rozendal *et al.* tested an MEC in two configurations, one with a Cation Exchange Membrane (CEM: also called as PEM) and one with an Anion Exchange Membrane (AEM), to examine the performance of MECs with different types of ion exchange membranes [9]. The schematic of these configurations is shown in Figure 4. The AEM allows the transport of anions from the cathode to the anode instead of the transport of cations. As demonstrated in Figure 4 for the MEC with the AEM, the hydrogen at the cathode is not produced from the reduction of protons but from the reduction of water. In this process, hydroxyl ions are produced equimolarly with the consumed electrons from the anode ($2 \text{H}_2\text{O} + 2 \text{e}^- \rightarrow 2 \text{OH}^- + \text{H}_2$). A comparison between the electrochemical cells of two configurations (applied voltage scans of the electrochemical cells) shows that at the lower applied voltage range, the CEM outperforms the AEM configuration. The CEM configuration starts to produce current (hydrogen) at applied

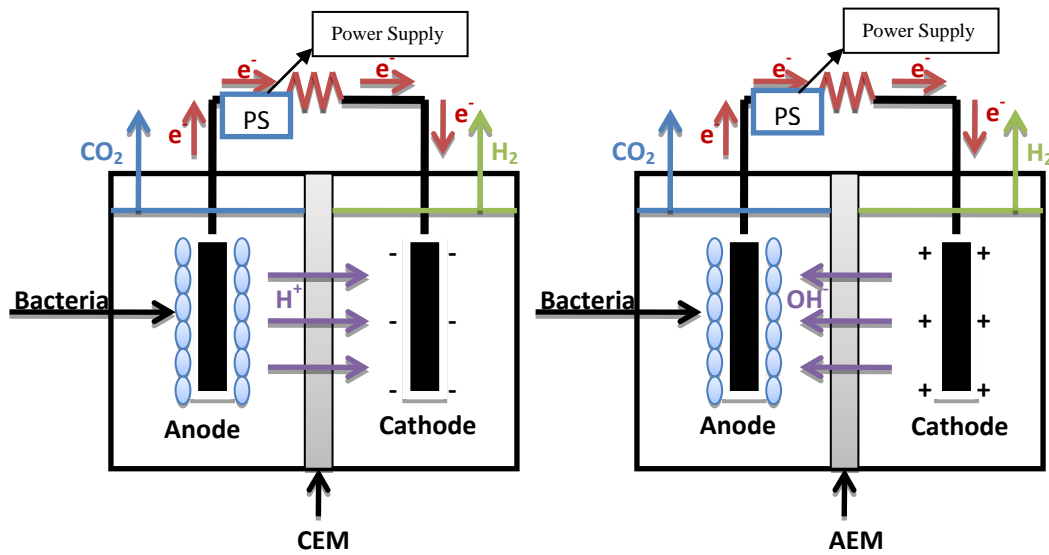


Figure 4: Schematic Representation of MEC with a CEM and an AEM [12]

voltages above 0.2V, while the AEM configuration starts to produce current at applied voltages above 0.4V [15]. However, at the higher applied voltages (1.0 V or above), the AEM configuration slightly outperforms the CEM configuration, even though it performs worse at the lower applied voltages. Both configurations demonstrated a comparable volumetric hydrogen production rate by producing over 0.3 m³ H₂/m³ reactor/day at 1.0 V of over potential applied. The pH gradient associated with the potential loss in the system is lower in the AEM configuration [9]; however, the potential losses associated with reduced pH gradient were negated by the increased cathode over-potentials as compared to the CEM configuration (CEM: 0.12 V at 2.39 A/m²; AEM: 0.27 V at 2.15 A/m²) [15]. In conclusion, it is possible to operate an MEC both with a CEM or an AEM and the CEM was found to be more suitable since the CEM outperforms at the lower applied voltages needed for a long operation cycle.

2.3 Power Density Measurements

To investigate MFC reactor performance and its efficiency at producing cell voltage or electricity, it is common to optimize the system for power production. The power output by an MFC is related to the measured voltage, E_{MFC} , across the external load and the current by $P=IE_{MFC}$ where the current can be relate to the external resistance R_{ext} by, $I = E_{MFC} / R_{ext}$. Hence the power can also be expressed as

$$P = E_{MFC}^2 / R_{ext} \quad (1)$$

There are many conventions for expressing the power density. In the literature, the power density may be calculated by dividing the power by the anode surface area, cathode surface area, membrane surface area or reactor liquid volume. It is important therefore to consider the volume or area units used to normalize the power when comparing MFC power generation results.

2.3.1 Power Output Normalized by Electrode Surface Area

Many researchers use the surface area of the anode for calculating power density; i.e.,

$$P_A = E_{MFC}^2 / (R_{ext} A_{An}) \quad (2)$$

This is because the amount of anode surface area available for microbes to grow can affect the amount of power generated. However this convention is not appropriate for all MFC system architectures. In systems where the anode is pressed onto a surface, only one side of the anode may be used (this is the projected surface area) [19, 12]. If both sides of the anode are suspended or exposed in a bacterium, both sides of the anode surface area may be used [20]. However, the surface of the anode does not always affect power generation. In some systems with very high anode surface area relative to the cathode area [7], it is more appropriate to normalize power generation by the cathode surface area.

2.3.2 Power Output Normalized by Membrane Surface Area

In reactor systems where a membrane separates the two electrode chambers, the membrane projected surface area may also be used to normalize the power [21]. According to Oh and Logan, power production can be affected by the relative sizes of the anode, cathode and PEM. A power density based on the membrane surface area is calculated as

$$P_A = E_{MFC}^2 / (R_{ext} A_{PEM}) \quad (3)$$

2.3.3 Power Output Normalized by Volume

The reactor liquid volume can also be used as a normalizing factor. Sometimes researchers normalized power production using the anode volume (based solely on geometry) or the anode liquid volume (excluding membrane area and gas head space) or total reactor volume (including both the cathode and anode chambers). If the cells are grown in a separate flask

outside the reactor and are recirculated through the anode, this volume may also be included. A volumetric power density based on the anode reactor volume is calculated as

$$P_v = E_{MFC}^2 / (R_{ext} V_{An}) \quad (4)$$

2.4 Internal Resistance

The internal resistance is one of the critical system variables to consider in MFC construction; high reactor internal resistance limits the performance of the MFC by limiting current supply within the system. Hence, it is important to understand, measure, and minimize the internal resistance to produce the maximum power output. Voltage output varies with external resistance, R_{ext} . The system components act as a second (internal) resistance, R_{int} , which can be considered to be in series with R_{ext} . Maximum power generation, P , often normalized by the volume of the anode, varies inversely with the total resistance of the system squared, $(R_{int} + R_{ext})^2$. While the R_{ext} can be varied, R_{int} is fixed. Therefore, P is ultimately limited by R_{int} . Substantially higher power densities can be achieved by using more efficient system architectures with lower internal resistances. These relationships are described below. The total current produced by an MFC is expressed as

$$I = E_{emf} / (R_{int} + R_{ext}) \quad (5)$$

where R_{int} is the internal resistance and R_{ext} is the external resistance in ohms. The open circuit voltage between the anode and cathode can be described as E_{emf} .

$$E_{emf} = IR_{int} + IR_{ext} \quad (6)$$

$$V = IR_{ext} \quad (7)$$

$$P = VI \quad (8)$$

$$P_{max} = IR_{ext} E_{emf} / (R_{int} + R_{ext}) \quad (9)$$

where E_{emf} is the electro-motive force of an MFC (open circuit voltage) in volts, V is the measured voltage (measured voltage) in volts, P is the power output in watts, and P_{max} is the maximum power output in watts. Hence, the maximum power output is inversely proportional to the square of total resistance:

$$P_{max} = E_{emf}^2 R_{ext} / (R_{int} + R_{ext})^2 \quad (10)$$

2.4.1 Measuring Internal Resistance

There are several different methods to evaluate the internal resistance of an MFC. These include the polarization slope method, the power density peak method, electrochemical impedance spectroscopy (EIS) using a Nyquist plot [22], and current interrupt methods [4]. In this study, the first two of these methods are used to estimate the internal resistance. As implied in the current equation described above, the polarization slope method uses a plot of current versus measured voltage, the slope of which is R_{int} . As long as the polarization curve is linear, the internal resistance is easily obtained over the region of interest. For the power density peak method, the maximum power occurs at the point where the internal resistance is equal to the external resistance. The internal resistance can therefore be calculated by determining the external resistance that produced the peak power output [4].

2.5 Preliminary Research

My research with MFCs concentrated on developing more efficient reactor designs. In order to evaluate changes in reactor design and performance of the MFCs in a timely manner, I initially focused on electrical power generation instead of hydrogen production. MFCs are generally easier to operate and monitor due to the simplicity of measuring electric energy production compared to collecting and analyzing a gas. MFC (for electricity production) and

MEC (for H₂ production) systems share many characteristics; therefore methods for improving electricity generation in MFCs will lead to increased hydrogen production in MECs.

The first MFC reactor I constructed was the H-type reactor in Figure 5A. The reactor was tested for power generation using a pure culture of *Shewanella oneidensis* MR-1 and produced up to 117 mW/m² referenced to the anode projected area. In this H-type design the anode and cathode chambers were connected by a narrow tunnel formed by two glass slip joints with a PEM membrane separating the chambers and with the electrodes suspended in an aqueous solution on either side of the PEM. While it was an easy reactor to construct and assemble, it had several design flaws that made it difficult to optimize the reactor performance; these include a large electrode separation, a large “dead volume” in the head space, small electrode and membrane areas compared to a large reactor volume, a large amount of bacterium trapped in the narrow membrane joint, and a poor system for feeding substrate and sampling the reactor solution. In order to eliminate these flaws, I constructed a sandwich-type miniature reactor

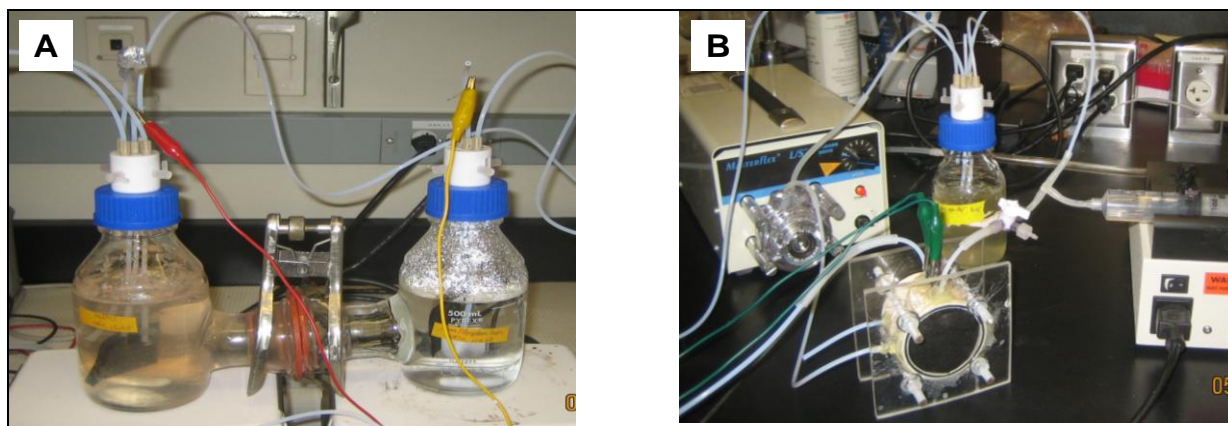


Figure 5: Types of MFCs used in the Previous Research - (A) H-type MFC Reactor Design (B) Sandwich-type MFC Reactor Design [Photograph courtesy of Dr. Ying Wang]

shown in Figure 5B based on the design of Bretschger et al. 2007 [18]. It was fabricated from PVC pipe material and was separated by a PEM. This reactor design allowed for following improvements:

- Elimination of the narrow membrane joint between two chambers so the anode and cathode are in direct contact with the membrane reducing the electrode spacing
- Reduction of the reactor volume by reducing the size of anode and cathode chambers; in particular making the cathode chamber half the size of the anode
- Complete packing of the anode chamber with anode electrode material (carbon felt) to provide a large anode electrode surface area, eliminating “dead volume” in the head space
- Continuous flow of substrate-containing medium across the biofilm on the anode side, enabling a consistent voltage production
- Use of an air-cathode instead of aqueous-cathode to eliminate a buffer solution

2.5.1 Comparison of MFC Reactor Types

2.5.1. A Voltage Production

The electrical energy generating abilities of H-type and sandwich-type MFC reactors were compared using a pure culture of *Shewanella oneidensis*, in a minimal medium (pH = 7.0) with lactic acid as the carbon substrate. The MFCs were traditionally operated at pH values between 6 and 8. The effect of pH on the growth and electron transfer abilities of *S. oneidensis* MR-1 in MFCs was examined and found in the literature [28]. The power density at neutral pH was significantly higher for *S. oneidensis* MR-1 in the mini-MFC using graphite felt electrodes and nanoporous polycarbonate membranes with *S. oneidensis* MR-1 [28]. Their work determined

that MFC performance was most efficient between pH 7 and 8 for *S. oneidensis* MR-1. Thus, *S. oneidensis* MR-1 growth at pH 7 was used in the study. 2 mM lactate was continuously fed into the 15 ml anode compartment in the sandwich-type reactor while 20 mM lactate was periodically fed into the 500 ml anode compartment in the H-type reactor in fed-batch fashion.

A month of experimentation demonstrated that the sandwich-type reactor outperformed the H-type reactor producing about 264 mV at 500 ohms of resistance within a week of operation. The H-type reactor reached its highest voltage on the 24th day of operation (Figure 6). In these experiments, the sandwich-type reactor provided a maximum volumetric power density of 9.3 W/m³ per anode liquid volume compared to 0.24 mW/m³ per anode liquid volume in the H-type reactor. This result indicated that the sandwich-type reactor was more efficient than the H-type reactor. This is likely due to the increased anode surface area per unit volume of the anode

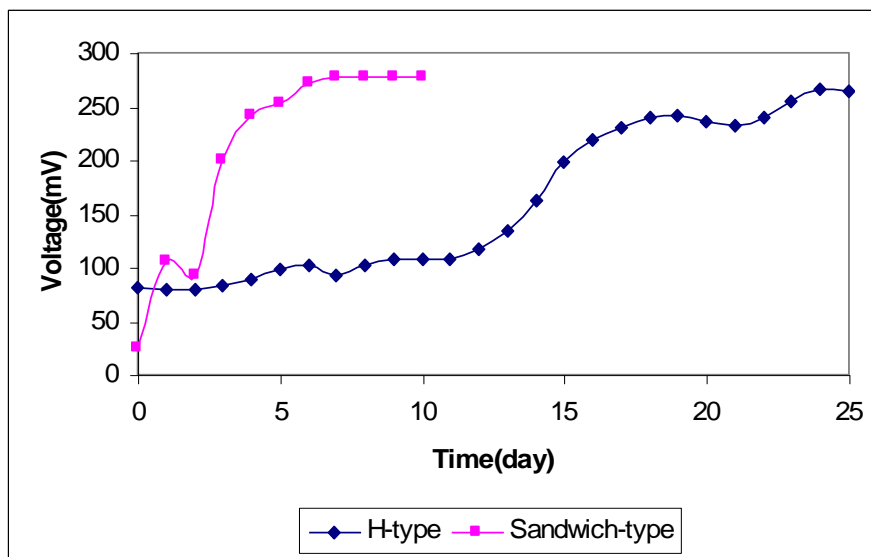


Figure 6: Comparison of Operation Efficiency on Voltage Generation between H-type and Sandwich-type Reactors at 500 ohms

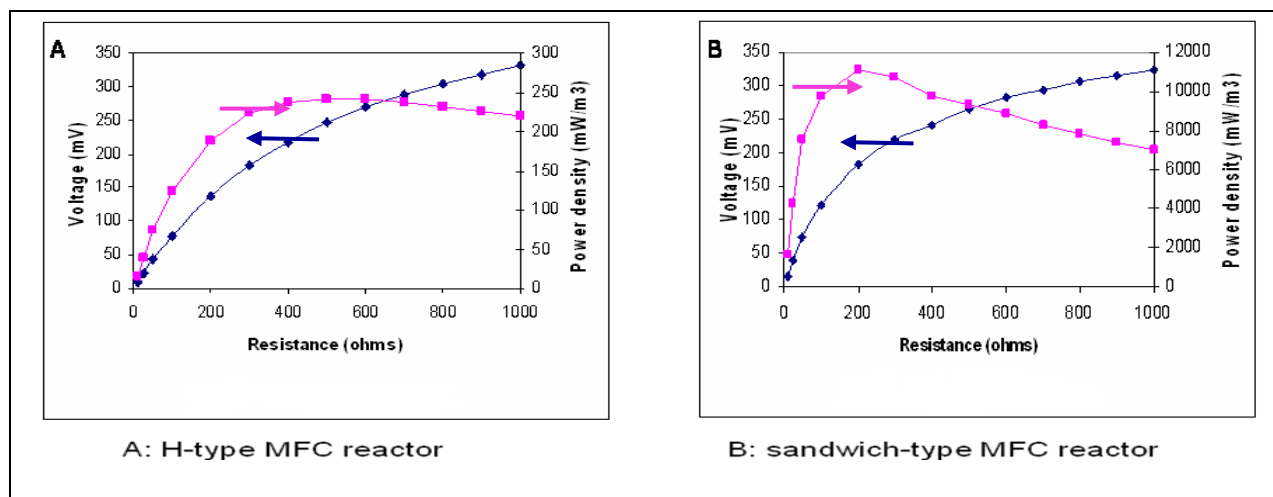


Figure 7: The Voltage Output and Power Density as a Function of the External Resistance - (A) H-type MFC reactor design (B) sandwich-type MFC reactor design, the power density was normalized by the reactor volume of the anode chamber

chamber with a low internal resistance caused by the small anode to cathode distance. The combined use of packed layers of graphite felt for the anode (high surface area), an increased size of the PEM with respect to reactor volume in a mini sandwich-type reactor, and small electrode spacing resulted in improved performance.

2.5.1. B External Resistance

In order to measure the power density as a function of resistance the external resistance across the anode and cathode was varied from 0 to 1,000 ohms (Figure 7). The voltage output increased with increasing external resistance in both H-type and sandwich-type reactors. As shown in Figure 8, the power density of the H-type reactor increased slowly with the resistance over the range of 0 to 500 ohms then steadily decreased after the maximum power density of 0.24 W/m³ at 500 ohms. The power density of the sandwich-type reactor showed a dramatic

increase in the range of 0 to 200 ohms of resistance. It reached a maximum value of 11 W/m^3 at 200 ohms after which it decreased monotonically.

CHAPTER 3

MATERIALS AND METHODS

3.1 Double-Anode Chambered Microbial Fuel Cell (MFC) Construction

In order to improve MFC performance and increase power density and hydrogen production rate a new MFC reactor design utilizing dual anode chambers was designed and constructed. This design has two advantages over more conventional designs. First, the provision of two anodes increases the maximum current over single anode designs. Second, close electrode spacing (2 cm) minimizes internal resistance, which should increase the maximum power output as maximum power output is produced at the smallest internal resistance (Figure 9). Other advantages associated with this dual-anode chambered MFC system include increased mass (proton) transfer to the single cathode chamber by sharing one common cathode, overall decreases in reactor volume and cathode material costs, and more simplified and convenient design structure. The working liquid volume of the anodic compartment is 15mL. The system was also designed to avoid voltage reversals as it operates under continuous flow mode, with the medium containing sufficient substrate passed sequentially through the reactor [18]. Substrate concentration and bacterial substrate consumption rate were continuously monitored and analyzed by high performance liquid chromatography (HPLC) (Waters, Alliance 2690 Analytical HPLC) of the filter sterilized growth medium. According to the literature, voltage reversal (the reversal in polarity of one or more cells and a loss of power generation) results when one cell does not generate sufficient voltage relative to other cells as the result of substrate starvation. It often occurs in stacked MFCs which are connected in series and operated under fed-batch mode [23]. In long term operation of MFCs, it is important to avoid two crucial voltage reversal factors,

substrate starvation and series electrical connectivity. In order to avoid these, the electrodes need to be connected in parallel and sufficient substrate needs to be provided to the anode [24]. The parallel electrical connectivity also helps to increase the electric current generation. A schematic that illustrates the continuous flow system of substrate and gas in the dual-anode chambered MFC is shown in Figure 8.

The dual-anode chambered system was operated in two different ways. One way was to generate electricity using an aerobic cathode and the other was to produce pure hydrogen gas using an anaerobic cathode. Pure hydrogen gas was evolved using the potential from the bacteria and a small additional applied voltage. In the hydrogen production configuration protons and electrons produced by bacteria are catalytically recombined at the cathode to form hydrogen gas.

An air-cathode was used for electricity generation; this allows the cathode to remain aerobic without having to sparge water with air in the cathode chamber. Oxygen, protons, and

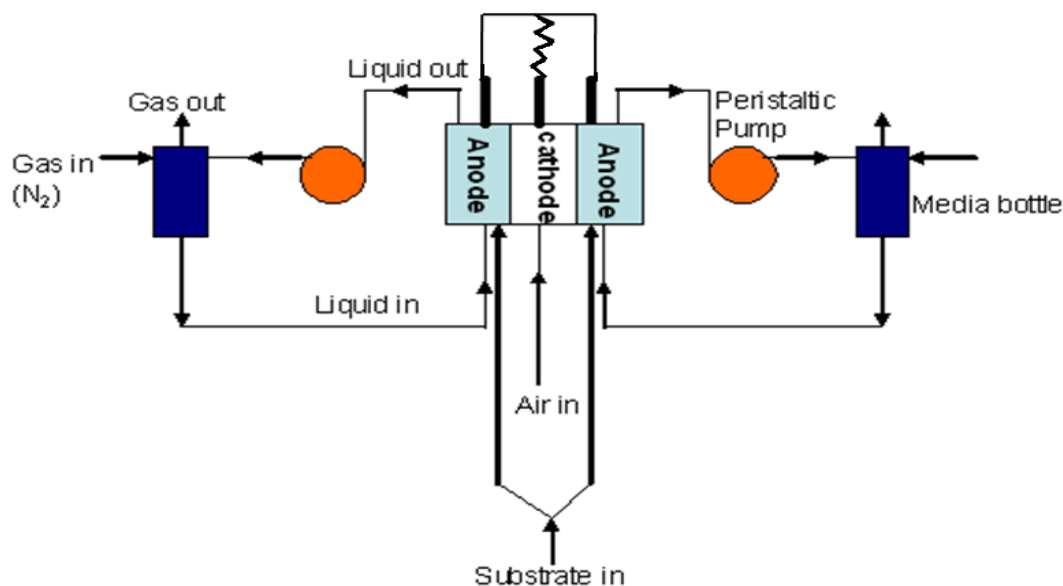


Figure 8: Schematic Diagram of Continuous Flow System of the Dual-Anode Chambered MFC

electrons are catalytically combined in the presence of a platinum catalyst to form water at the cathode chamber and generate electricity. Figure 9 shows a miniature dual-anode chambered MFC that was used for electricity generation. However, this reactor design could be operated as either an MFC or MEC based on whether air (to the cathode chamber) and additional voltage are added to the system. Thus it can be switched between these two modes of operation.

3.2 MFC Reactor Design Materials and Features

The dual-anode chambered MFC consists of three separate chambers: two anaerobic anode chambers inoculated with a pure bacterial culture, *S. oneidensis*, and a cathode chamber where electricity or hydrogen is produced. The anode and cathode chambers were fabricated from transparent polycarbonate material (lexan pipe, anode chamber size: 5 cm diameter, 2.54 length, cathode chamber size: 5 cm diameter, 1.27 cm length) and were separated by the PEM (Nafion: Alfa Aesar, size: 5 cm diameter), which was fitted in between two rubber gaskets. The PEM was pretreated by boiling in a solution of deionized water and H₂O₂ (30%), followed by H₂SO₄ and deionized water, each for 1 h, and then was stored in deionized water prior to being used. Solid graphite rods were used as the cathode and anode electrodes and the two anodes were connected electrically in parallel using copper wires. The anodes were placed close to the cathode to reduce internal resistance. The anodic compartments were filled with carbon felt to increase the surface area available to bacteria for transferring electrons. At the cathode, the graphite carries electrons to the final electron acceptor; when operated aerobically, the final electron acceptor is oxygen. Increasing the surface of the anode relative to that of the cathode can increase power by increasing the number of bacteria adhered to the carbon felt allowing the

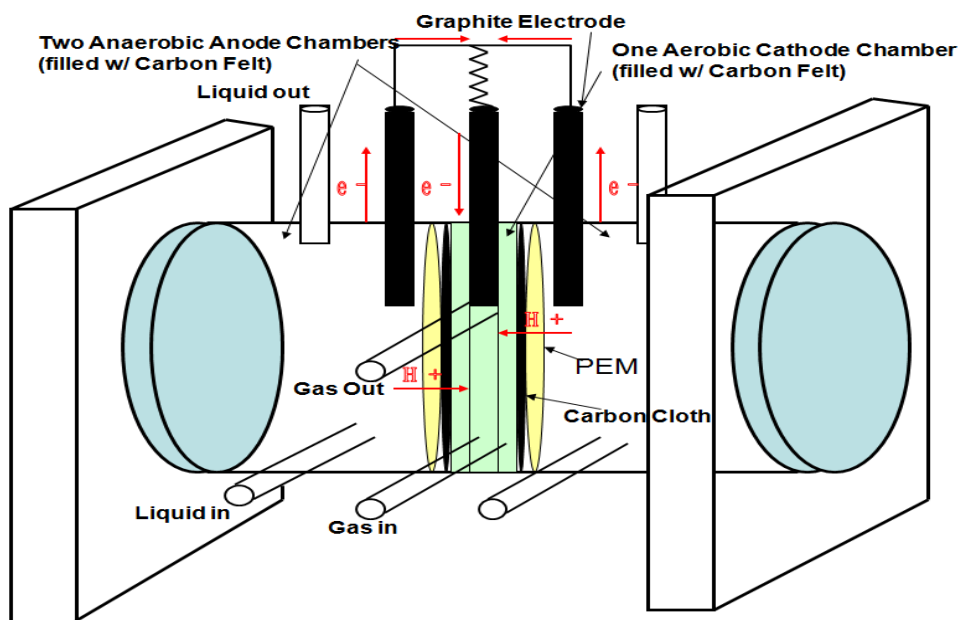
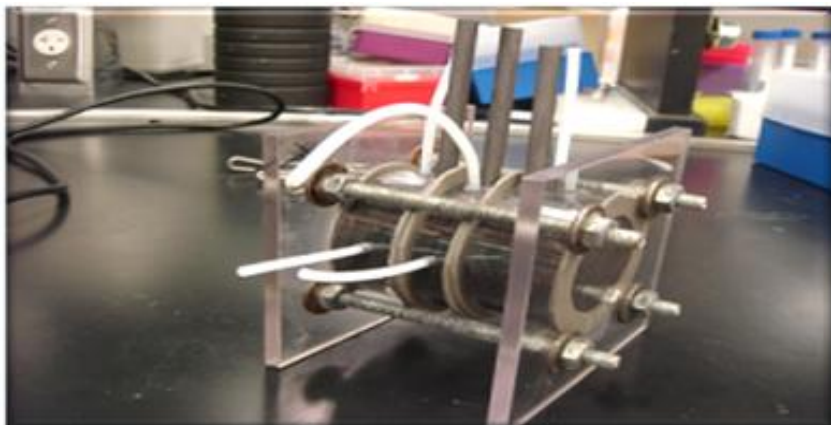


Figure 9: Representation of Mini Dual-Anode Chambered MFC for Electricity Generation

formation of a larger biofilm, which increases the generation of electrons and their transfer. Carbon cloth impregnated with platinum metal (Fuel cell store, 2cm x 3cm) was used as the cathode material and it was pressed against the PEM. This arrangement should reduce or eliminate transport resistance through a fluid phase and should provide a fast transfer of protons across the PEM.

3.3 Culture and Medium

A pure culture of *S. oneidesis* MR-1 was used as the inoculum in the anode compartment of the MFC. The *S. oneidesis* MR-1 strain was stored at -80 °C prior to use. The Defined Medium for *Shewanella* (DMS) from Galit Meshulam-Simon *et al.* 2007 [25] was used for all experiments and contained: 5.7mM K_2HPO_4 , 3.3mM KH_2PO_4 , 125mM NaCl, 5.4 μ M $FeCl_2 \cdot 4H_2O$, 5 μ M $CoCl_2 \cdot 6H_2O$, 485 μ M $CaCl_2 \cdot 2H_2O$, 5 μ M $NiCl_2 \cdot 6H_2O$, 9mM $(NH_4)_2SO_4$, 0.2 μ M $CuSO_4$, 1mM $MgSO_4$, 1.3 μ M $MnSO_4$, 1 μ M $ZnSO_4$, 57 μ M H_3BO_3 , 67.2 μ M Na_2EDTA , 3.9 μ M Na_2MoO_4 , 1.5 μ M Na_2SeO_4 , 2mM $NaHCO_3$, and a vitamin mixture (1 L of medium contains 0.02 mg biotin, 0.02 mg folic acid, 0.1 mg pyridoxine HCl, 0.05 mg thiamine HCl, 0.05 mg riboflavin, 0.05 mg nicotinic acid, 0.05 mg DL-pantothenic acid, 0.05 mg p-aminobenzoic acid, 0.05 mg lipoic acid, 2mg choline chloride, 0.01mg vitamin B12). Sterilized sodium DL-lactate at experiment-specific concentrations was used as the carbon source. Sodium DL-lactate was sterilized by filtration. The medium was adjusted to a pH of range 6.8 to 7.2 by addition of 1M NaOH. The inoculation loop was used to pick a single colony from the plate and inoculate in a small test tube containing an LB broth medium and grown overnight at 33 °C temperature. Then the grown cells in the test tube were re-inoculated into 20ml of LB broth medium in a

shake-flask and grown overnight at 33 °C temperature. The following day, the grown cells were centrifuged (4000 rpm for 15min) and the cell pellet was washed three times in a DMS solution. The washed cells were re-suspended in the DMS solution to the desired cell concentration, estimated by reading optical density using spectrophotometer set to 600nm (OD_{600}); the desired concentration range was between 0.1 and 0.2.

3.4 Hydrogen Production using a Dual-Anode Chambered MEC

The dual-anode chambered MEC reactor (for hydrogen production) design in Figure 10 includes the following features: H_2 gas collector, continuous-feeding flow of medium and substrate into each anode chamber, and continuous monitoring systems for cell voltage and hydrogen production. For both the MEC and MFC the voltage across a load was measured and recorded every 1 min by a data acquisition box (National Instruments, NI USD-6221), using a Labview (National Instruments) program running on a personal computer. A steady-state voltage production was reached after 5 days. Three replicate reactors were used and the experimental measurement for each reactor was taken and the average value was used. An H_2 sensor [31] (Figure 11) was built and used for monitoring hydrogen production. At the beginning of experiments I was primarily focused on electrical power generation from MFCs for evaluating the changes and improvements in the design structure and the reactor performance. As mentioned earlier, MFCs producing electricity do not require the collection and analysis of a gas product and so were easier to operate for purposes of optimizing the design. Hydrogen production experiments were conducted by using the optimized solution from the electrical power generation experiments.

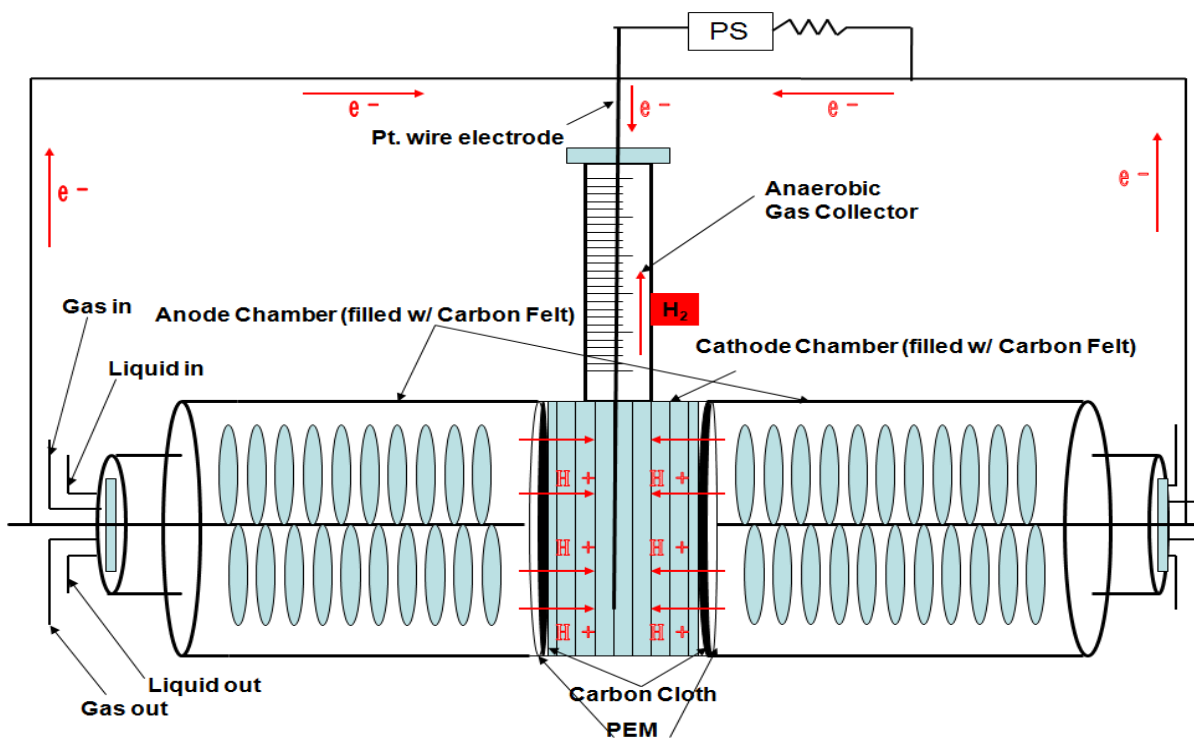


Figure 10: Representation of a Dual-Anode Chambered MEC for Hydrogen Production

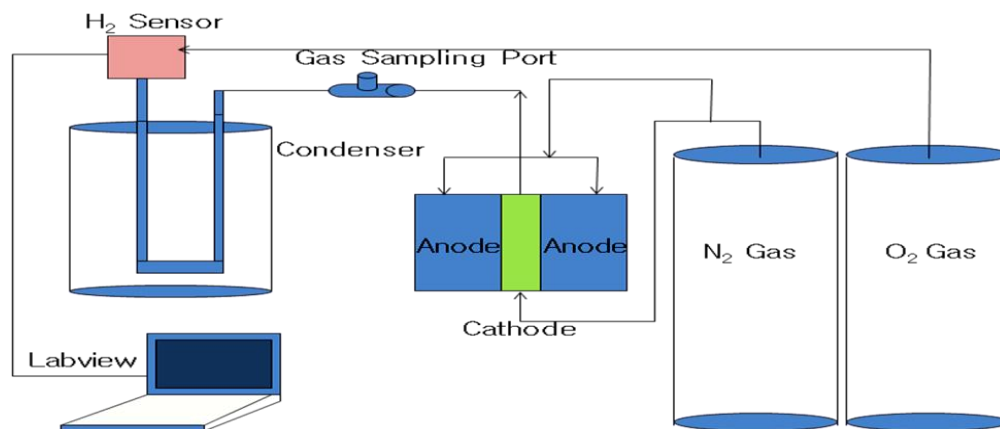


Figure 11: Schematic Representation of the Experimental Apparatus for Hydrogen Production [Courtesy of Donglee Shin] – A carrier gas, flowing at 50 ml/min entered cathode chamber of the MFC. Hydrogen produced in the MFC reactor (cathode) was transported to the hydrogen sensor by the carrier gas. Output from the hydrogen sensor was sent to a personal computer via Labview program

3.5 Operational Conditions

A series of miniature dual-anode chambered MFCs were constructed and were operated at room temperature (approx. 22°C). These were used to compare electricity production while varying experimental parameters for improving electricity generation (Figure 9). The fact that power generation is so sensitive to the sizes of PEM, electrode spacing, and other factors makes it essentially impossible to know if one bacterium can produce more power than another, if power is affected by substrate of medium composition and concentration, or if power is affected by the use of different catholytes, unless all variables and parameters were tested in the same system. Therefore, it was important that all parameters and variables must be varied in otherwise identical conditions in order to quantify the effect of these parameters on the operation of MFCs/MECs.

3.5.1 Experimental Variables

In this study, I examined the effect of several system variables on power, power density, and hydrogen production. For power production, the following variables were measured: cell potential, volumetric power density, internal resistance, and current. For hydrogen production, volumetric hydrogen production rate, hydrogen yield per substrate, and coulombic hydrogen recovery (coulombic efficiency) were measured.

3.5.2 Experimental Parameters

The external resistance, substrate concentration, substrate flow rate, and cathode surface area were varied in order to study their effects on reactor performance and product efficiency for generating electricity and hydrogen. For hydrogen production, an applied voltage of 0.5V was used. While varying external resistance from 20 to 1000 ohms, the voltage was monitored and used to determine the maximum volumetric power density for power generation.

The substrate feed rate affects bacterial growth on the anode electrode and thus the power output was monitored while varying the flow rate of substrate and medium. In this study, lactate was selected as the growth substrate and used to evaluate the growth of *S. oneidensis* MR-1. Previous studies of *S. oneidensis* MR-1 reported that the lactate can be used as a primary carbon source for *S. oneidensis* MR-1 to generate electric current in a minimal medium [27]. This is because *S. oneidensis* MR-1 prefers three-carbon carbohydrates for growth. Experimentally, L-lactate, pyruvate, and acetate are among compounds utilized as sources of carbon and energy [30]. To investigate the effects of bacterial activity on cell voltage production, different lactate concentration (5, 10, and 20 mM) and different flow rates (1, 3, and 5ml/min) were tested and evaluated.

Different sizes of cathode surface areas were also used and compared to investigate reactor performance. In some systems with very high anode surface areas relative to the cathode areas, some literature normalized their power densities using the cathode surface areas [7]. In this study I used a rectangular shaped cathode electrode material, plantinized carbon paper (cloth), in sizes (length x width) of 4cm x 3cm and 2cm x 3cm.

CHAPTER 4

RESULTS AND DISCUSSION

4.1 Dual-Anode Chambered MFCs for Electricity Production

4.1.1 Effect of Cathode Surface Area on Power Generation

The voltages produced using the same cathode system with different total cathode surface areas (12 cm^2 vs. 24 cm^2) were compared and examined in MFC tests (Figure 12, Table 1 and Table 2). The carbon paper pre-loaded with a Pt catalyst was used as the cathode material. Nafion was used as a PEM material due to its high proton conductivity and as a cathode binder to allow the transfer of protons and electrons to the cathode electrode in an air cathode system in the dual-anode chambered MFCs. As Figure 12 shows, increasing the cathode surface area of Pt-coated electrode by 100% to 24 cm^2 produced no difference in voltage compared to the case when the cathode surface area was 12 cm^2 . These results demonstrated that the surface area of

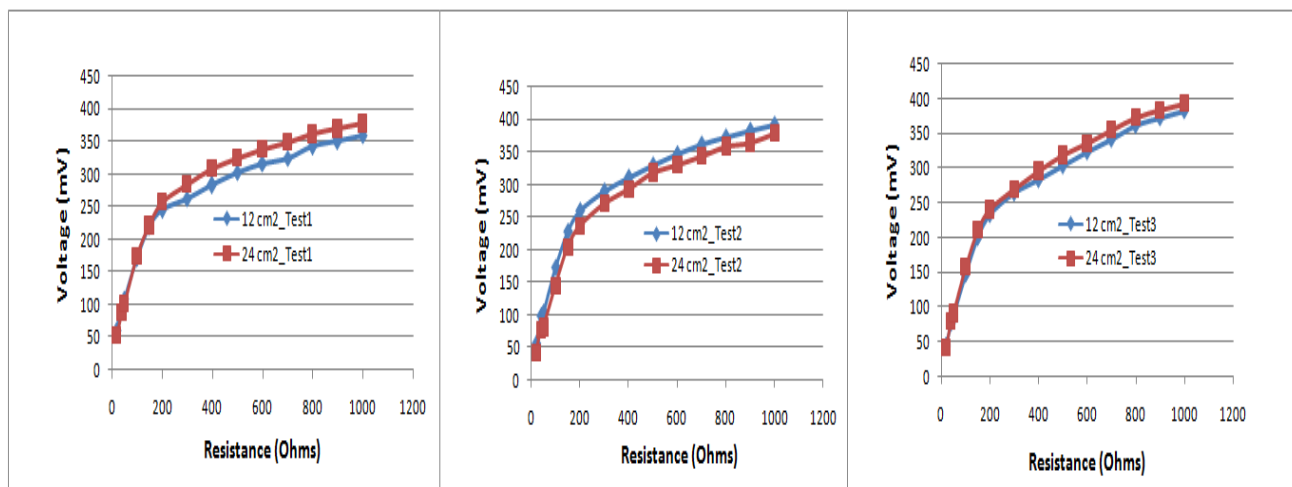


Figure 12: Representation of Voltage Production at Different Total Cathode Surface Areas - Comparison Experiments Run In Triplicate

Table 1: Effect of Cathode Surface Area on Maximum Power Generation with 5 mM Lactate Concentration

Maximum Power Output (mW)						
Total Cathode S.A (cm ²)	Test 1	Test 2	Test 3	Avg (mW)	S.D	Error
12	0.320	0.344	0.271	0.312	0.037	0.022
24	0.326	0.281	0.297	0.301	0.023	0.013

Table 2: Effect of Cathode Surface Area on Voltage Production with 5 mM Lactate Concentration

Voltage Production at 200 ohms (mV)						
Total Cathode S.A (cm ²)	Test 1	Test 2	Test 3	Avg (mV)	S.D	Error
12	245	259	233	246	13.01	7.51
24	257	237	241	245	10.58	6.11

the cathode in the certain experimental range of 12 – 24 cm² does not limit power generation in the dual-anode system.

4.1.2 Power generation as a Function of Substrate Concentration

When lactate was added to the MFC, the current or power density increased to a plateau value (Figure 13B). The rates of current increment were proportional to lactic acid concentration over the range of 5 - 20mM. Since a current was produced by the addition of the natural electron donors (lactate) of the bacterium, it could be concluded that the bacterial oxidation of the electron donors and the direct electron transfer from the cell surface to electrode produced the electrochemical signals.

Following inoculation with *S. oneidensis* MR-1, a stable voltage was generated after adding a different substrate concentration of lactate, 5 mM (450 mg/l), 10mM (900 mg/l), and 20mM (1800 mg/l) into the anode chambers. A plot of the volumetric power density at each

initial substrate concentration demonstrated saturation kinetics (Figure 13B). When fit to saturation kinetics, a half-saturation constant K_s of 6.15mM and an R^2 of 0.902 were obtained. A maximum power density of P_{\max} , 11.6 W/m³ was obtained using 5 mM lactate, while those using 10 mM and 20 mM lactate concentrations were P_{\max} =18.3 W/m³ and P_{\max} =18.5 W/m³ (Figure 13B). Since many researchers use different ways of optimizing their maximum power output based on their reactor system architectures, I normalized the maximum power production by anode and cathode electrode surface areas, by membrane surface area, and by total reactor liquid volume and anode inoculation liquid volume. These values are shown in Table 3. It was found that 20 mM lactate achieved the highest maximum power output of the three lactate concentrations. However, 10 mM lactate also resulted in a very similar power density value to 20 mM lactate. Therefore, 10 mM lactate was determined to be an effective operational substrate concentration by considering the amount of substrate required to feed into the reactor. A maximum volumetric power density based on the anode liquid volume at each substrate concentration was obtained in Figure 13A.

4.1.3 Effect of Substrate and Medium Flow Rates on Power Generation

Current cannot be generated in an MFC at a rate greater than the rate bacteria can oxidize a substrate and transfer electrons to the electrode surface. As bacteria colonize a surface and form a biofilm, the rate of substrate consumption by the biofilm can eventually exceed mass transfer to the surface. Using continuous flow mode, the relationship between maximum growth rate and substrate flow rate was investigated with lactate as the limiting factor of a culture of *S. oneidensis* MR-1. Here we considered the possibility that substrate flux to the biofilm limits power generation by determining the effective substrate flow rates at 1ml/min, 3ml/min and

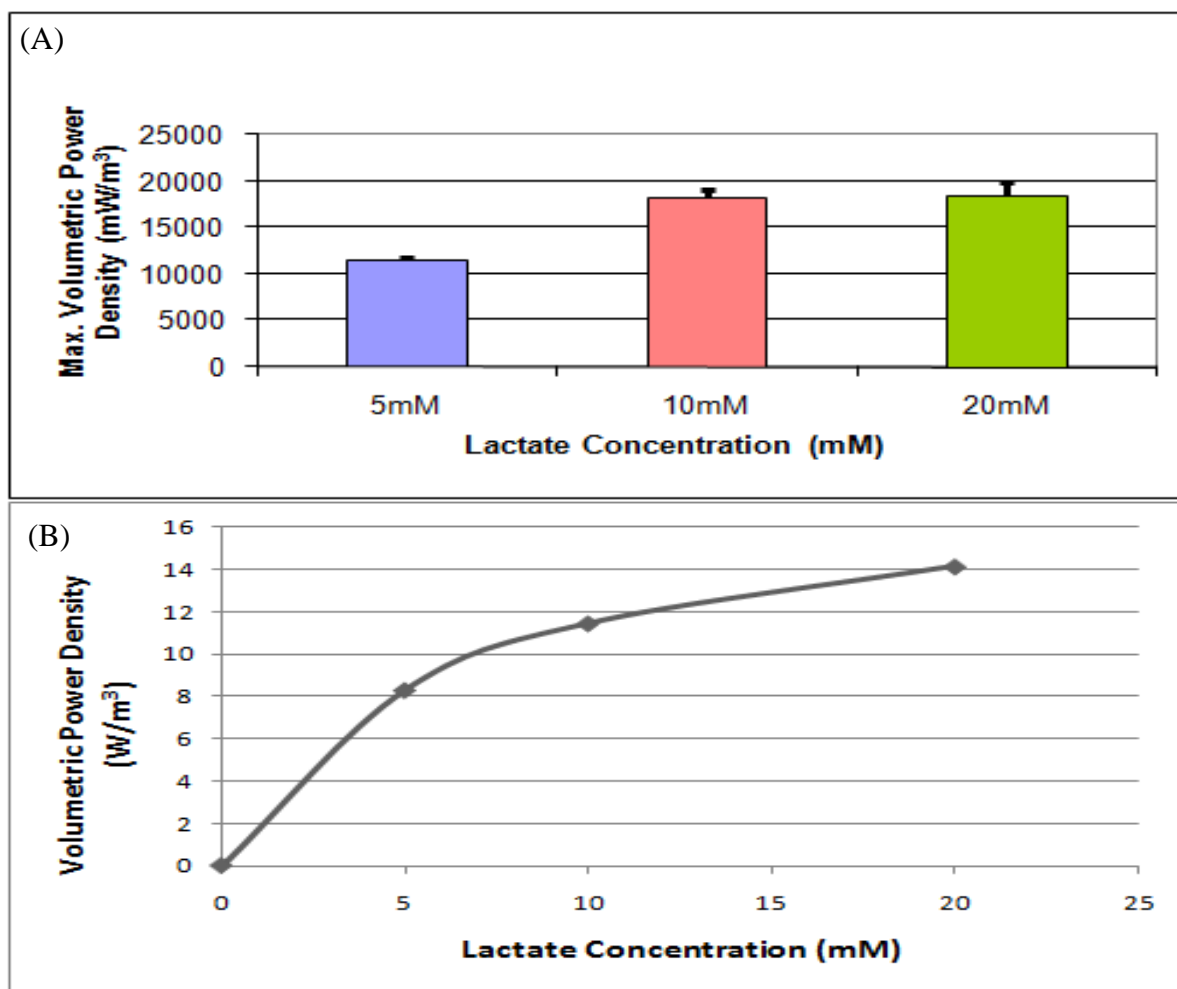


Figure 13: Volumetric Power Density at each Lactate Concentration - (A) Maximum volumetric power density as a function of lactate concentration with error bars and SD based on the maximum power densities in experiments run in triplicate (B) Plot of saturation kinetics using Michaelis-Menten kinetic model with $K_s = 6.15$, $R^2 = 0.902$

Table 3: Maximum Power Density Normalized By Different Parameters at Each Lactate Concentration

Lactate Conc. (mM)	Max. Power Production (mW)	Max. PD_An (W/m ²)	Max. PD_Cat (mW/m ²)	Max. PD_Mem (mW/m ²)	Max. PD_An_Vol. (W/m ³)	Max. PD_Total Vol. (W/m ³)
5	0.347	85.6	289	85.6	11.6	1.24
10	0.549	136	458	136	18.3	1.96
20	0.555	137	462	137	18.5	1.98

5ml/min. The maximum volumetric power density was obtained at each flow rate by using operational conditions of 10 mM lactate concentration (Figure 14), 12 cm² of cathode surface area (Table 1), and 15ml of anode liquid volume based on the previous experiments. The most effective substrate feed rate on the MFC occurred at 5 ml/min and it produced its maximum volumetric power density in respect to anode liquid volume as 23.6 W/m³. Power densities of 18.3 W/m³ and 17.7 W/m³ were achieved for substrate flow rates of 3 ml/min and 1 ml/min, respectively. The MFC with the optimized flow rate of 5 ml/min produced approximately 22 % higher power density compared to 3 ml/min. When 10 mM lactate was used as the carbon source in a dual-anode MFC system, the average doubling time during the exponential growth phase in fully anaerobic conditions was approximately 11 h, much slower than the 3 h doubling time observed for aerobic growth with 50 mM lactate in Tang et al., 2006 [29]. Maximum growth rates of 0.0263, 0.0640, and 0.0745 hr⁻¹ were achieved for initial substrate flow rates of 1ml/min, 3ml/min, and 5ml/min, respectively. An average substrate consumption rate for *S. oneidensis* MR-1 in an anaerobic dual-anode system was found to be approximately 5.5 mM lactate consumed per day (0.23 mM lactate per hour) or 20.6 mg lactate consumed per hour and growth on lactate was saturated at a concentration greater than 20 mM.

4.1.4 Comparison of Single-Anode Chambered and Dual-Anode Chambered MFC Performance

The maximum power generation (W/m³) under optimized operational conditions was obtained and used to compare the reactor performance of the dual-anode chambered MFC with an existing reactor configuration using a single-anode chamber (Figure 15). The voltage and

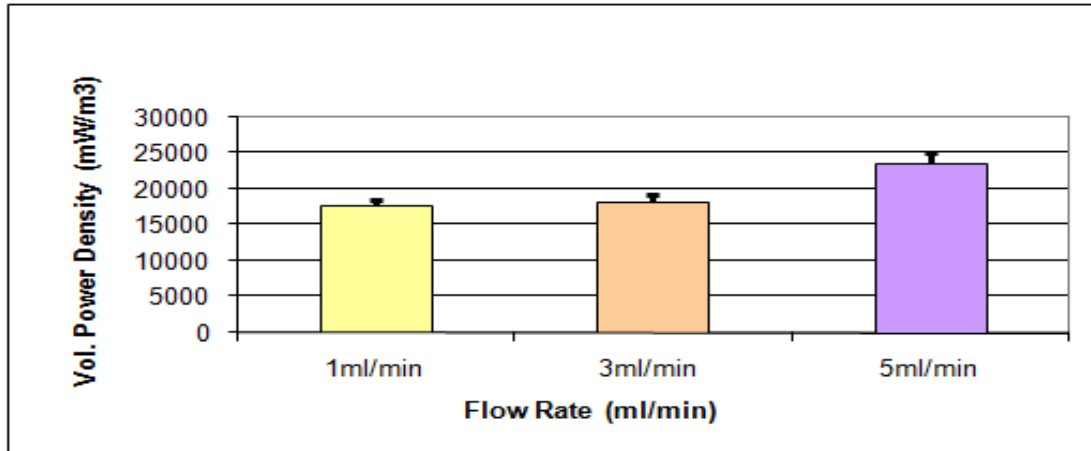


Figure 14: The Effect of Substrate and Medium Feed Rates on Power Density

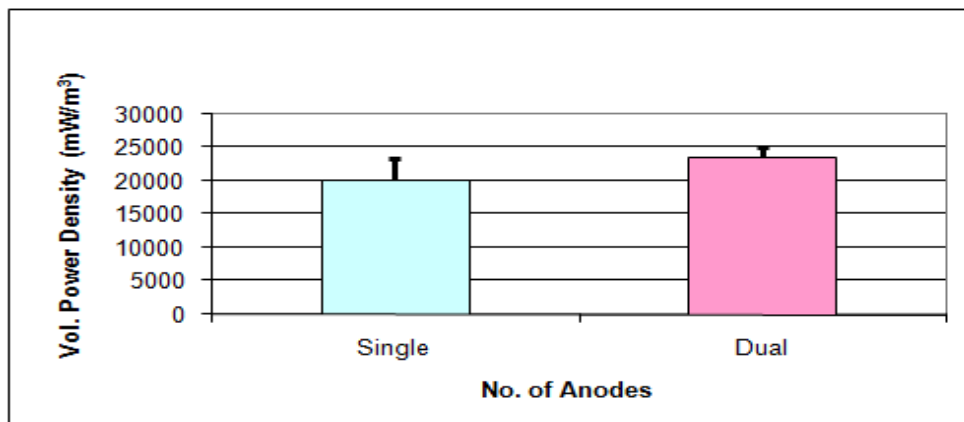


Figure 15: Comparison of Maximum Power Generation on Single-Anode and Dual-Anode Chambered MFCs under Optimized Operational Conditions at 5 ml/min Flow Rate, 10 mM Lactate

volumetric power densities obtained using single-anode chambered MFCs were generally lower than those produced by dual-anode chambered MFCs. An average voltage output produced by single-anode system was 0.226 V and 0.314 V was obtained by the dual-anode system (200 Ω external resistances). To determine what load (resistance) would produce the maximum power density the circuit resistance was varied from 20 to 450 Ω with optimized operational conditions. The maximum power from the single-anode MFC reached 20.3 W/m³ (standard deviation: 4.43, error: 2.56), producing a current of 1.69 mA (100 Ω) (Figure 16, 17). The MFC with dual-anode chambers generated 23.6 W/m³ (standard deviation: 2.25, error: 1.3) with a current of 3.66 mA (50 Ω).

The higher current achieved here was possibly due to the reduction of internal resistance within the system. As Figure 18 illustrates, the internal resistance can be evaluated by using the polarization slope method, as it was described in section 2.5.1 (Measuring internal resistance). The slopes of the polarization curve for single and dual MFC systems were linear over the range of 0.65 – 2.6 mA, Figure 18 (A) and 1.3 – 5.2 mA, Figure 18B, respectively. The internal resistance (slope) was determined to be 106 Ω for the single-anode MFC and 58.3 Ω for the dual-anode MFC system, which is a reduction of 45% for the dual-anode system. For the power density peak method, the internal resistances yielded 100 Ω for the single and 50 Ω for the dual (Figure 16), which is quite similar to that obtained from the first approach of using polarization slope method. The reactor configuration of dual-anode chambers played a critical role in the reduction of the total resistance of the system by having reduced electrode spacing and by providing parallel electrical connectivity. Since the internal resistance of the MFC was primarily

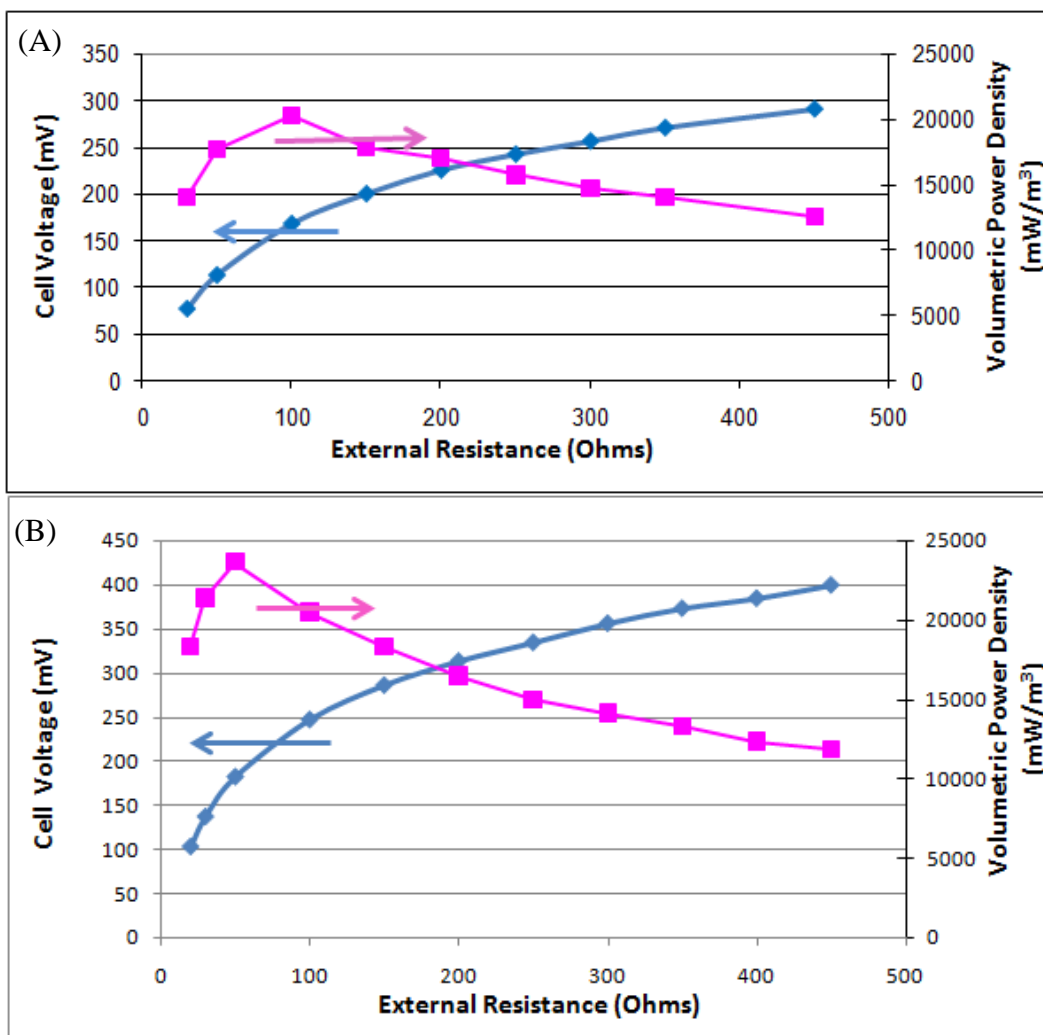


Figure 16: Power Density and Cell Voltage Curves - By switching out the circuit load; we obtain a data set on the cell voltage and the volumetric power density as a function of resistance (A) Single-Anode Chambered MFC (B) Dual-Anode Chambered MFC

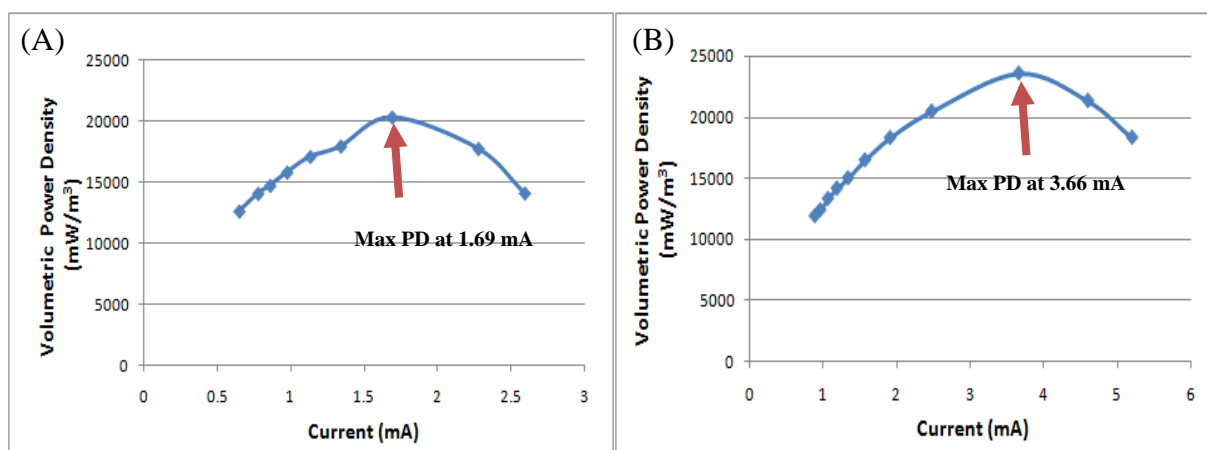


Figure 17: Power Density Generated as a Function of Current - (A) Single-Anode Chambered MFC (B) Dual-Anode Chambered MFC

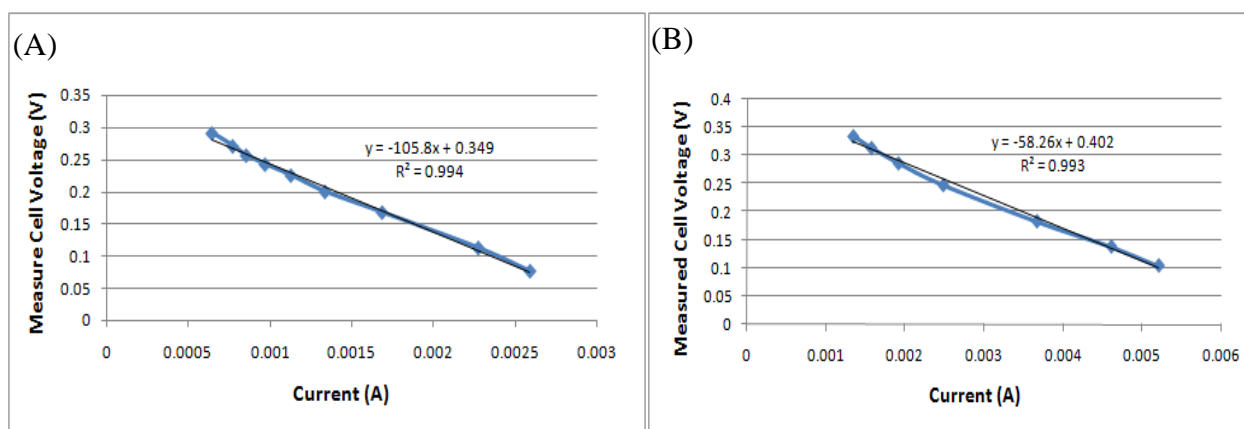


Figure 18: Polarization Curves - Cell voltage versus Current to obtain the polarization curve showing the regions of constant voltage drop (A) Single-Anode Chambered MFC (B) Dual-Anode Chambered MFC

a function of electrode spacing [9], the internal resistance of the dual-anode chambered MFCs was substantially lower than the single-anode chambered MFC.

Ohm's law states that the current in a circuit is inversely proportional to the circuit resistance. The amount of current is determined by the total resistance of the circuit (internal and external resistances) and the measured cell voltage. In a parallel circuit the source current divides among the available electrical paths or number of anodes in our system. Hence, the dual-anode chambered MFC can yield the higher current by lowering internal resistance. For the same voltage rating, a larger MFC (dual-anode chambered) tends to have a larger amount of stored charge and be able to supply higher current for a given time (Amp). The amount of charge passing through a point over a given period of time produces an electric current such that

$$I = Q/t$$

where I is the current in amps, Q is charge in coulombs and t is time in seconds.

4.2 Dual-Anode Chambered MECs for Hydrogen Production

Hydrogen gas was produced with dual-anode chambered MECs when current generation was forced by applying a small external voltage (> 0.2 V in practice) between the anode and the cathode, causing hydrogen gas to be produced at the anaerobic cathode through the reduction of protons. In this study, I used optimized operational conditions that were determined in the power generation experiments described above. These operational conditions were included 10mM of lactate concentration, 5 ml/min of substrate flow rate, and the cathode surface area of 12cm^2 . The amount of hydrogen produced per mol substrate consumed was used as the hydrogen yield. The maximum hydrogen yield was 0.438 mol H_2 per mol substrate at an applied voltage of 0.5V using 10 mM lactic acid, with a production rate of $0.165 \text{ m}^3 \text{ H}_2$ per m^3 reactor per day, based on

the anode liquid volume. Using lactate, an average substrate consumption rate of 2.19 mM/day was determined. For this specific substrate, the theoretical number of moles of hydrogen that could be produced by complete oxidation of the substrate was 4.6×10^{-3} mol H₂ per day. The total moles of hydrogen recovered based on the measured current was determined as 3.36×10^{-4} mol H₂ per day, and the coulombic hydrogen recovery or the total recovered moles of H₂ vs. the theoretically possible was found to be 7.3%. Based on the electrical power production using the same operational conditions, the molar yield of hydrogen per substrate can also be predicted assuming 100% cathode conversion efficiency as 0.851 mol H₂/mol substrate, which is double the amount of hydrogen produced by an MEC. This calculation can be achieved using the maximum current (3.66 mA) produced by the dual-anode chambered MFC (Figure 17B) and an average substrate consumption rate of 5.12 mM per day which was obtained in the dual-anode chambered MFC for electricity production.

The low recovery of hydrogen achieved in the MEC experiment in comparison with the theoretical hydrogen recovery was thought to be due to the overpotentials associated with the pH gradient. The transport of cation species other than protons across the PEM may have caused a pH increase in the cathode chamber. As the Nernst equation states, every pH unit difference between anode and cathode increases the equilibrium potential E_{eq} by about 0.06 V, which requires additional energy (applied energy) in order to generate hydrogen in the MEC [14]. This may help explain why bacteria like *S. oneidensis* MR-1 that produce acetate and hydrogen, cannot further convert the remaining acetate to hydrogen completely. Based on the HPLC analysis, acetate was found as one of the end products from lactate metabolism by *S. oneidensis* MR-1. According to the literature, the major products of lactate metabolism are acetate and

pyruvate, with over 70% of the lactate being converted to acetate, pyruvate, and succinate under anaerobic growth of *S. oneidensis* MR-1 in lactate minimal medium [32].

CHAPTER 5

CONCLUSIONS

Dual-anode chambered MFCs exhibit higher current production than single-chambered MFCs. The internal resistance of the MFC was significantly lower in the dual-anode configuration (two chambers flanking a single cathode chamber) compared to the single anode. This was achieved by reducing the spacing between electrodes and by providing parallel electrical connectivity. The dual chambered MFC displayed a maximum volumetric power density of 23.6 W/m^3 when operated in continuous flow mode under optimized operating conditions. This was higher than 20.2 W/m^3 , the maximum power density achieved by the single-anode chambered MFC. The internal resistance was reduced by 45% from 106Ω (single-anode) to 58.3Ω (dual-anode), which indicated that a dual-anode produces about twice as much current per unit anode volume as a single-anode (3.66 mA and 1.69 mA , respectively).

As discussed in the introduction, it was expected that hydrogen productivity in the MEC would be optimized at the same conditions where electrical energy production was optimized. However, the dual-anode chambered MEC design operated at an applied voltage of 0.5 V demonstrated volumetric hydrogen production rate of $0.165 \text{ m}^3 \text{ H}_2$ per m^3 anode liquid volume per day and a hydrogen yield of 0.438 mol H_2 per mol substrate. These values were lower than the values ($2.01\text{-}3.95 \text{ mol H}_2/\text{mol substrate}$, $1.1 \text{ m}^3 \text{ H}_2/\text{m}^3 \text{ reactor/ day}$ at applied voltages of 0.2 to 0.8 V using acetic acid) obtained from the hydrogen production by bacterial fermentation of glucose [7], but the volumetric hydrogen production rate was greater than the rate ($0.02 \text{ m}^3 \text{ H}_2/\text{m}^3 \text{ reactor/day}$ at an applied voltage of 0.5 V) found using a H-type MFC [14].

LIST OF REFERENCES

1. Liu, H., R. Ramnarayanan, and B.E. Logan, *Production of electricity during wastewater treatment using a single chamber microbial fuel cell*. Environmental Science & Technology, 2004. **38**(7): p. 2281-2285.
2. Oh, S., B. Min, and B.E. Logan, *Cathode performance as a factor in electricity generation in microbial fuel cells*. Environmental Science & Technology, 2004. **38**(18): p. 4900-4904.
3. Logan, B.E. and J.M. Regan, *Microbial challenges and applications*. Environmental Science & Technology, 2006. **40**(17): p. 5172-5180.
4. Logan, B.E., *Microbial fuel cells*. 2008, Hoboken, N.J.: Wiley-Interscience. xii, 200.
5. Lower, S.K., M.F. Hochella, and T.J. Beveridge, *Bacterial recognition of mineral surfaces: Nanoscale interactions between Shewanella and alpha-FeOOH*. Science, 2001. **292**(5520): p. 1360-1363.
6. Bond, D.R. and D.R. Lovley, *Electricity production by Geobacter sulfurreducens attached to electrodes*. Applied and Environmental Microbiology, 2003. **69**(3): p. 1548-1555.
7. Cheng, S., H. Liu, and B.E. Logan, *Increased power generation in a continuous flow MFC with advective flow through the porous anode and reduced electrode spacing*. Environmental Science & Technology, 2006. **40**(7): p. 2426-2432.
8. Cheng, S. and B.E. Logan, *Sustainable and efficient biohydrogen production via electrohydrogenesis*. Proceedings of the National Academy of Sciences of the United States of America, 2007. **104**(47): p. 18871-18873.
9. Rozendal, R.A., H.V.M. Hamelers, and C.J.N. Buisman, *Effects of membrane cation transport on pH and microbial fuel cell performance*. Environmental Science & Technology, 2006. **40**(17): p. 5206-5211.
10. Kim, J.R., et al., *Power generation using different cation, anion, and ultrafiltration membranes in microbial fuel cells*. Environmental Science & Technology, 2007. **41**(3): p. 1004-1009.
11. Chae, K.J., et al., *Mass transport through a proton exchange membrane (Nafion) in microbial fuel cells*. Energy & Fuels, 2008. **22**(1): p. 169-176.
12. Liu, H. and B. Logan, *Electricity generation using an air-cathode single chamber microbial fuel cell (MFC) in the absence of a proton exchange membrane*. Abstracts of Papers of the American Chemical Society, 2004. **228**: p. U622-U622.
13. Liu, H., S.A. Cheng, and B.E. Logan, *Production of electricity from acetate or butyrate using a single-chamber microbial fuel cell*. Environmental Science & Technology, 2005. **39**(2): p. 658-662.
14. Logan, B. *Microbial Fuel Cell Research*. 2007 Dec.19 2007 [cited 2008 Aug. 8 2008].
15. Rozendal, R.A., et al., *Performance of single chamber biocatalyzed electrolysis with different types of ion exchange membranes*. Water Research, 2007. **41**(9): p. 1984-1994.
16. Call, D. and B.E. Logan, *Hydrogen production in a single chamber microbial electrolysis cell lacking a membrane*. Environmental Science & Technology, 2008. **42**(9): p. 3401-3406.
17. Rozendal, R.A., et al., *Principle and perspectives of hydrogen production through biocatalyzed electrolysis*. International Journal of Hydrogen Energy, 2006. **31**(12): p. 1632-1640.

18. Bretschger, O., et al., *Current production and metal oxide reduction by Shewanella oneidensis MR-1 wild type and mutants*. Applied and Environmental Microbiology, 2007. **73**(21): p. 7003-7012.
19. Liu, H., S.A. Cheng, and B.E. Logan, *Power generation in fed-batch microbial fuel cells as a function of ionic strength, temperature, and reactor configuration*. Environmental Science & Technology, 2005. **39**(14): p. 5488-5493.
20. Min, B.K., S.A. Cheng, and B.E. Logan, *Electricity generation using membrane and salt bridge microbial fuel cells*. Water Research, 2005. **39**(9): p. 1675-1686.
21. Logan, B.E., et al., *Biological hydrogen production measured in batch anaerobic respirometers (vol 36, pg 2530, 2002)*. Environmental Science & Technology, 2003. **37**(5): p. 1055-1055.
22. Manohar, A.K., et al., *The use of electrochemical impedance spectroscopy (EIS) in the evaluation of the electrochemical properties of a microbial fuel cell*. Bioelectrochemistry, 2008. **72**(2): p. 149-154.
23. Oh, S.E. and B.E. Logan, *Voltage reversal during microbial fuel cell stack operation*. Journal of Power Sources, 2007. **167**(1): p. 11-17.
24. Shin, S.H., et al., *Development of bipolar plate stack type microbial fuel cells*. Bulletin of the Korean Chemical Society, 2006. **27**(2): p. 281-285.
25. Meshulam-Simon, G., et al., *Hydrogen metabolism in Shewanella oneidensis MR-1*. Applied and Environmental Microbiology, 2007. **73**(4): p. 1153-1165.
26. Bretschger, O., et al., *Current production and metal oxide reduction by Shewanella oneidensis MR-1 wild type and mutants (vol 73, pg 7003, 2007)*. Applied and Environmental Microbiology, 2008. **74**(2): p. 553-553.
27. Kim, H.J., et al., *A microbial fuel cell type lactate biosensor using a metal-reducing bacterium, Shewanella putrefaciens*. Journal of Microbiology and Biotechnology, 1999. **9**(3): p. 365-367.
28. Biffinger, J.C., et al., *The influence of acidity on microbial fuel cells containing Shewanella oneidensis*. Biosensors & Bioelectronics, 2008. **24**(4): p. 900-905.
29. Tang, Y.J.J., A.L. Meadows, and J.D. Keasling, *A kinetic model describing Shewanella oneidensis MR-1 growth, substrate consumption, and product secretion*. Biotechnology and Bioengineering, 2007. **96**(1): p. 125-133.
30. Serres, M.H., et al., *Genomic analysis of carbon source metabolism of Shewanella oneidensis MR-1: predictions versus experiments*. Journal of Bacteriology, 2006. **188**(13):p. 4601-4609
31. Millsaps, J.F., et al., *Nanoscale photosynthesis: Photocatalytic production of hydrogen by plantinized photosystem I reaction centers*. Photochemistry and Photobiology, 2001. **73**(6):p. 630-635
32. Tang, Y.J., et al., *Anaerobic central metabolic pathways in Shewanella oneidensis MR-1 reinterpreted in the light of isotropic metabolite labeling*. Journal of Bacteriology, 2007. **189**(3):p. 894-901

VITA

Min Hea Kim was born in Seoul, South Korea on March 3, 1982. She and her family moved to Perth, Australia in May 1999. She spent four years of high school years there and graduated from Kingsway Christian College (High School) in Perth, Western Australia in December of 2001. She attended University of Tennessee, Knoxville and received a Bachelor of Science from the Department of Chemical Engineering in December, 2006. She entered graduate school in August 2007 at the University of Tennessee, Knoxville. In May, 2009, she will receive a Master of Science from the Department of Chemical and Biomolecular Engineering.